

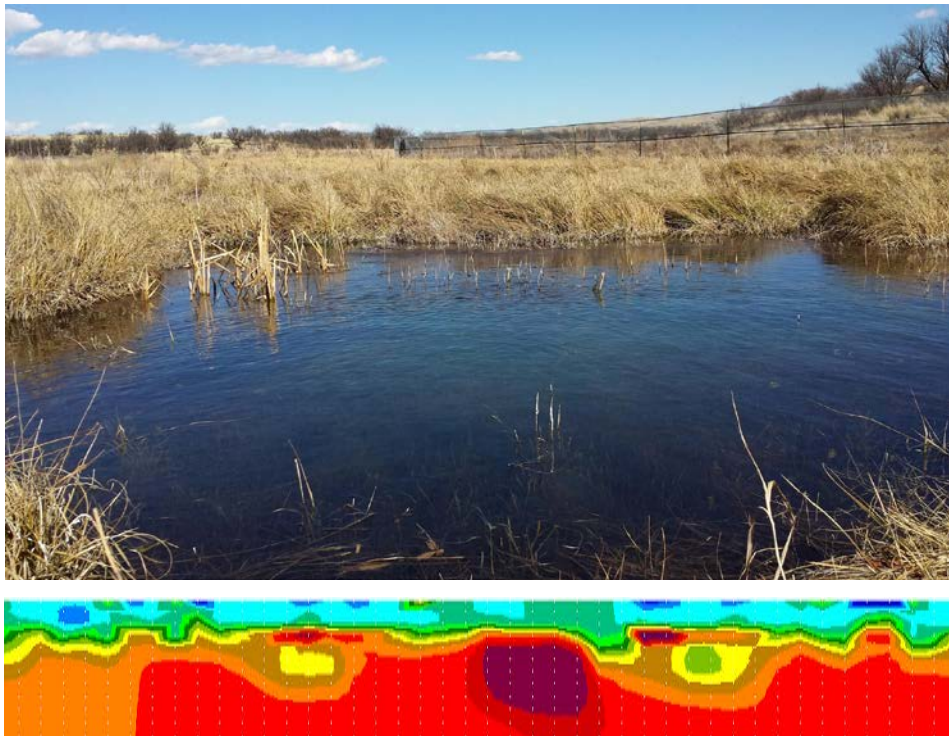
Near-Surface Geophysics Surveys at Empire Gulch in the Las Cienegas Conservation Area, SE Arizona

Geophysics Field Camp 2017

Laboratory for Advanced Subsurface Imaging
LASI-17-1

July 6, 2017

Daniel Basabe, Riley J. Burkart, Erica A. Cupp, Patrick O. Dougherty,
Libby Kahler, Dr. Ben K. Sternberg, Rachel S. Tucci, Thomas D. Tuten



Abstract

Electrical resistivity and induced polarization surveys were conducted in the Las Cienegas National Conservation Area for the Nature Conservancy and in accordance with the Bureau of Land Management. Data collected around Empire Ranch HQ shows a thin, high resistivity layer at the surface underlain by a lower resistivity layer, indicative of typical regional alluvium. H0 and H1 show resistivity of approximately 80 Ω -m down to 5 and 10 meters, underlain by 25 Ω -m and 20 Ω -m respectively. H2 and H3 shows resistivity of 60 Ω -m down to 5 and 15 meters, respectively, underlain by 20 Ω -m resistivity. Moving east, the data displays a distinct change. A thin, high-resistivity surface layer is underlain by an extremely low resistivity layer, typical of clays. H5, Z2 and H6 display surface resistivity between 20 Ω -m and 15 Ω -m, typical alluvium values. The massive underlying layer displays resistivity values of approximately 5 Ω -m. Continuing east, H7 shows a thick layer of high (80 Ω -m) resistivity surface material down to 25 meters, underlain again by a massive, low resistivity layer with a typical clay value of 5 Ω -m. H8 and Z3, collected in the Cieneguita cienegas complex, both display a 5 Ω -m surface layer down to 5 meters, indicative of clays. The surface layer is underlain by a 15 Ω -m, low-porosity layer, essentially devoid of clays, interpreted as Late Tertiary and Quaternary basin fill.

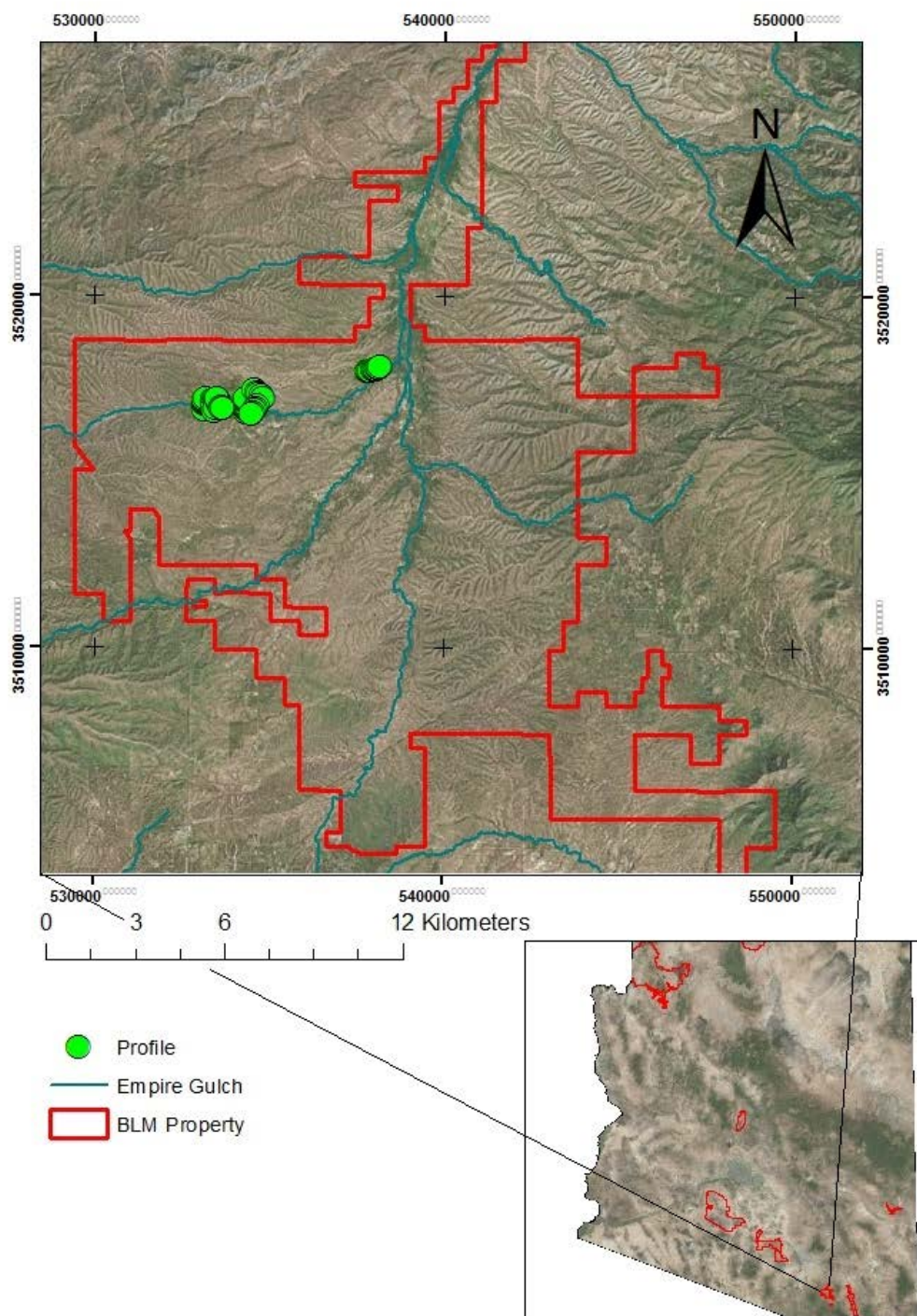
Table of Contents

	Page
ABSTRACT.....	2
TABLE OF CONTENTS.....	3
1. INTRODUCTION.....	5
2. METHODS	
2.1. INTRODUCTION.....	8
2.2. DC RESISTIVITY.....	8
2.3. INDUCED POLARIZATION.....	12
2.4. INVERSION.....	13
3. ZONGE SURVEY	
3.1. INTRODUCTION.....	15
3.2. ELECTRICAL SURVEY LOCATION.....	15
3.3. INSTRUMENTATION AND FIELD PROCEDURES.....	20
3.4. RESULTS.....	25
4. HYDROGEOPHYSICS SURVEY	
4.1. INTRODUCTION.....	43
4.2. ELECTRICAL SURVEY LOCATION.....	43

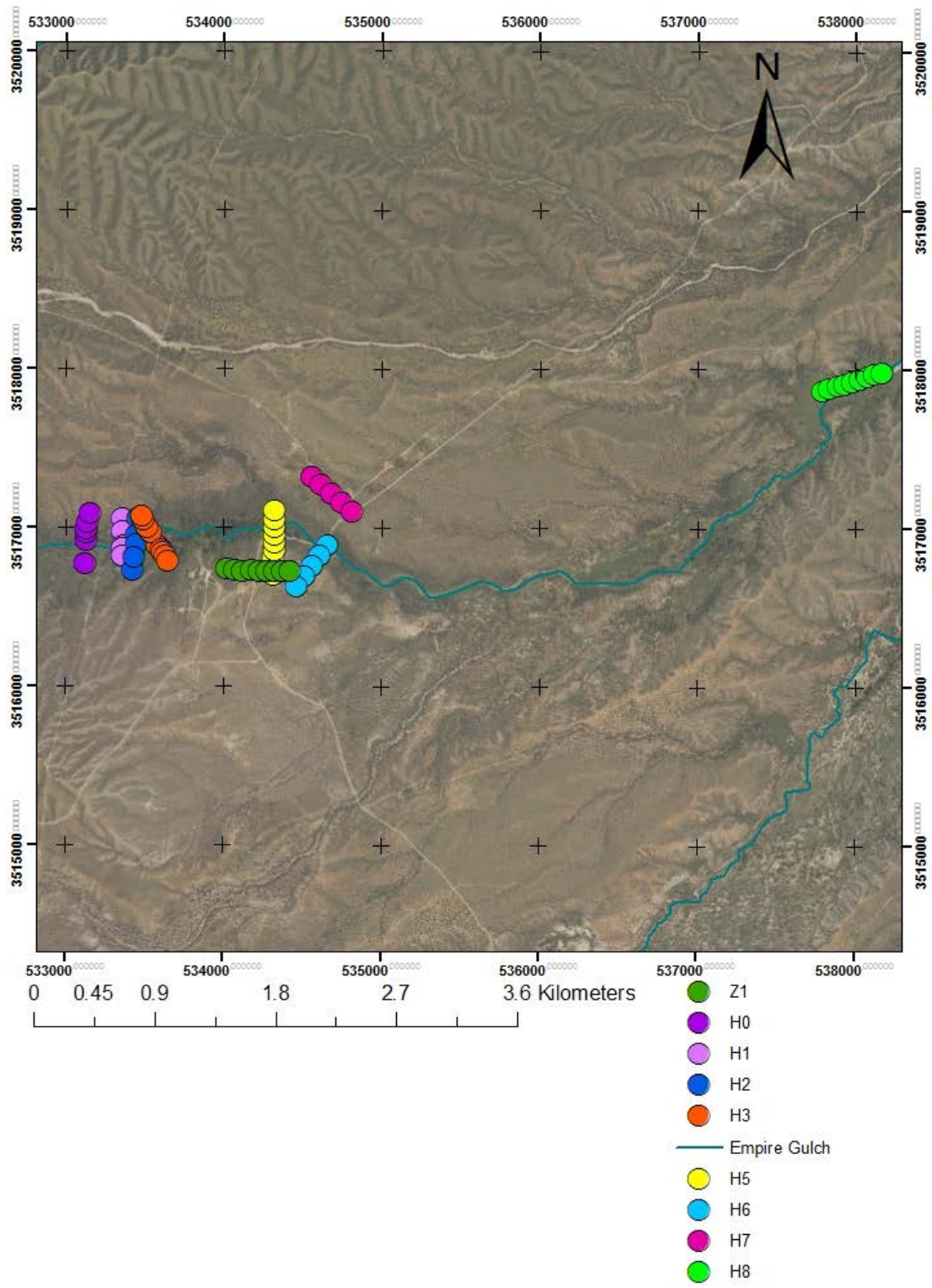
4.3.	INSTRUMENTATION AND FIELD PROCEDURES.....	50
4.4.	RESULTS.....	53
5. EMPIRE RANCH HEADQUARTERS		
5.1.	INTRODUCTION.....	61
5.2.	LOCATION.....	61
5.3.	SIDE-BY-SIDE COMPARISON.....	67
5.4.	PROJECTED RESISTIVITY CROSS SECTIONS.....	69
6. CIENEGUITA CIENEGA COMPLEX		
6.1.	INTRODUCTION.....	72
6.2.	LOCATION.....	72
6.3.	SIDE-BY-SIDE COMPARISON.....	76
6.4.	WELL LOGS.....	77
7. CONCLUSIONS.....		
7.1.	POSSIBLE FUTURE SURVEYS.....	82
8. ACKNOWLEDGEMENTS.....		
9. REFERENCES.....		
		85

1. Introduction

The Cienega Creek Watershed (CCW) of southeastern Arizona is a 600-square mile semi-arid alluvial basin. Cienega Creek and a major tributary to lower Cienega Creek Davidson Canyon are designated “Outstanding Arizona Waters”, which indicate superior water quality and provide habitats for threatened and endangered species of flora and fauna. Cienega Creek has two designated protected regions; the Las Cienegas National Conservation Area (LCNCA), managed by the Bureau of Land Management (BLM) in the upper portion of Cienega Creek, and the lower Cienega Creek, classified as a Natural Preserve and managed by Pima County Regional Flood Control District (RFCD). Increased demands on groundwater resources through land use of mining, urbanization and changes in climate could affect the quantity of available groundwater. The LCNCA is primarily used for ranch land, outdoor recreation, and scientific studies. The LCNCA area contains wetlands called cienegas that flank part of the upper Cienega Creek region. The cienegas are areas of interest because the scarcity of surface water features in this region limits the habitat for aquatic species, some of which are threatened. The amount and sustainability of groundwater flow to the cienegas is currently limited, and not completely understood. Issues of interest concerning the groundwater availability and flow include questions such as what geologic controls, like shallow bedrock or clay confining units, determine where the aquifer(s) in the subsurface are, and why do the cienegas form where they do? This study will use DC resistivity geophysical data around Empire Ranch HQ and the Cieneguita cienegas complex (Map 1.1-1.2) in the LCNCA to answer these questions. Resistivity is a measurement of the earth’s ability to resist electrical current. The greater the water content, the lower the resistivity values will be. The data are used to image the subsurface resistivity of earth materials (Zonge 2017). The results will be displayed in cross-sections with the intent to locate potential clay layers and/ or depth to water table. Additional well logs and geologic data will be used for interpretation of the measurements.



Map 1.1: Area of Interest.



Map 1.2: Profile of survey lines.

2. Methods

2.1 Introduction

Electrical methods in geophysics utilize currents, either natural or artificial, in the ground to map subsurface variations in electrical properties. Because these electrical properties are characteristic of different rock types, a survey using electrical methods can give insight into the geology of the area of interest. Two such methods, Direct Current (DC) Resistivity and Induced Polarization (IP), were used to survey the Cienega Creek area in this study. Both DC Resistivity and IP surveys were conducted using equipment from Zonge International, while the Hydrogeophysics Inc. equipment was only used for a DC Resistivity survey.

2.2 DC Resistivity

The DC Resistivity method relies on the injection of current into the ground, which results in differences in electric potential that are measurable at the surface. Extrapolating from the relation provided by Ohm's Law, a measured current and potential can be used to calculate the apparent resistivity ρ_a , the resistivity that would theoretically yield the measured values in an electrically homogenous and isotropic half-space. Resistivity ρ itself is defined as:

$$\rho = \frac{\delta R \delta A}{\delta L}$$

Where δR , δA , and δL are the respective resistance, cross-sectional area, and length of a solid (Figure 2.1).

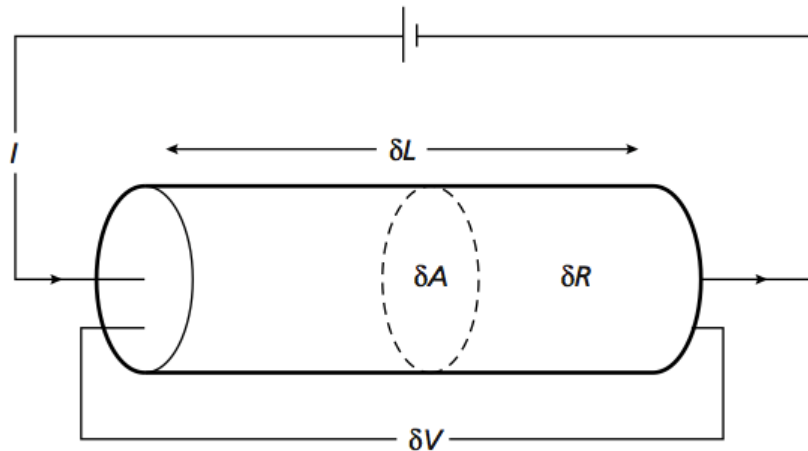


Figure 2.1 The parameters necessary to define resistivity for a solid cylinder (Kearey et al., 2002).

The resistivity of a material is an intrinsic property that describes the degree to which the material resists the flow of electric current. While certain minerals conduct currents very well, most rocks act as insulators, so current is conducted through the passage of ions in water-filled cracks and pores in the rock. As a result, the resistivity depends heavily on the porosity and water saturation of the rock, as shown in Archie's Law, an empirical formula for resistivity:

$$\rho = \frac{a\rho_w}{\varphi^m s_w^n}$$

Where a is an empirical constant, ρ_w is the resistivity of pore water, φ is the fractional porosity, s_w is the fractional water saturation, and m and n are empirical constants. Due to these factors, resistivity is a highly variable property, but certain rock types still exhibit approximate ranges of resistivity that can aid in identification (Figure 2.2).

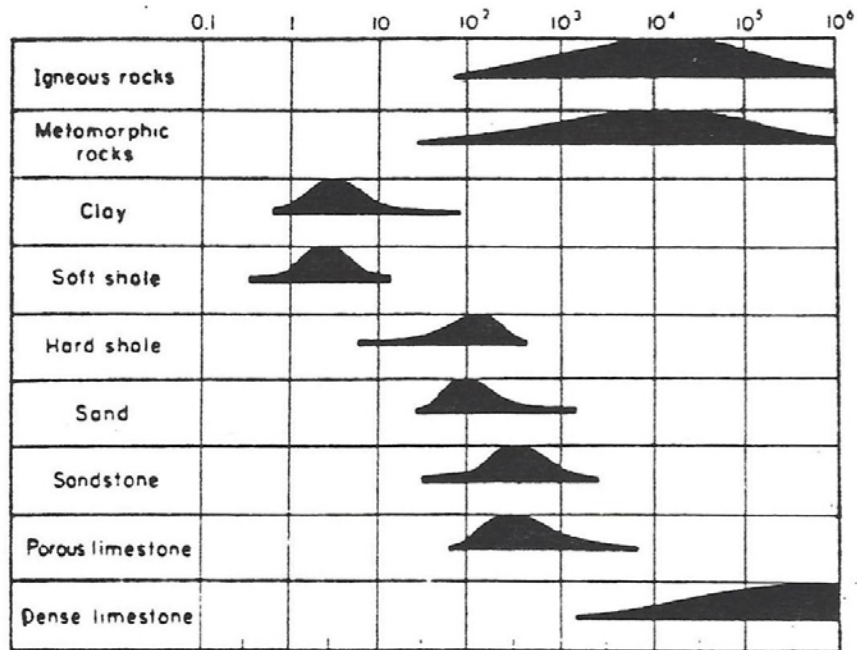
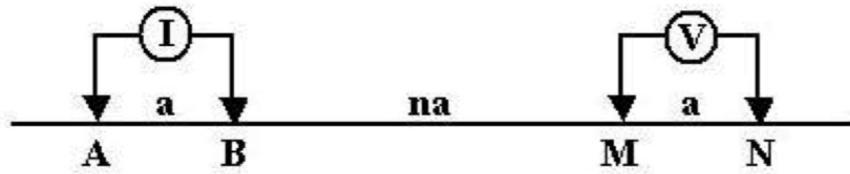


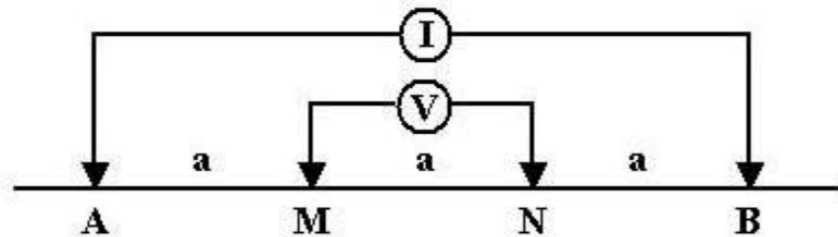
Figure 2.2. Approximate resistivity ranges for a number of rock types. Resistivities (in Ohm-m) are listed in a log scale on the horizontal axis (Sharma, 1986).

The exact process for calculating apparent resistivities from the measured currents and potentials depends on the geometry of the electrode configuration used to introduce the currents into the ground. Three such configurations were used in this study: the Dipole-Dipole Array, an altered Wenner Array, and the Schlumberger Array (Figure 2.3). The Zonge International equipment utilized the Dipole-Dipole Array, while the Hydrogeophysics Inc. equipment used a specially designed Wenner Array capable of collecting many more data points than the normal Wenner Array; a Schlumberger Array was also used for one profile line with the Hydrogeophysics equipment, due to time constraints.

(a)



(b)



(c)

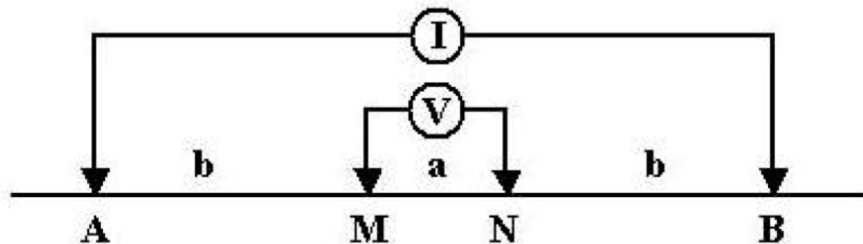


Figure 2.3 Arrays used to survey the Cienega Creek area: (a) Dipole-Dipole, (b) Wenner, and (c) Schlumberger. “I” represents the current source, “V” represents the measured potential, and A, M, N, and B represent the electrodes (Gasperikova and Morrison, 2016).

Despite the method’s name, it is important to note that a constant direct current is often not used, due to problems stemming from electrode polarization and telluric currents. Instead, direct

current is often introduced as a pulsed, square-waveform with alternating polarity; alternatively, a low frequency alternating current (AC) may also be used.

2.3 Induced Polarization

In a standard four-electrode DC Resistivity array, the introduced DC current is abruptly switched off to produce a pulsed, square waveform, but the measured potential decays gradually, rather than abruptly (Figure 2.4). This is because the ground acts as a natural capacitor, storing induced electrical charge that only gradually dissipates after the current is shut off. This phenomenon can be observed as either the transient dissipation of residual potential or variation in apparent resistivity as a function of the frequency of an introduced alternating current.

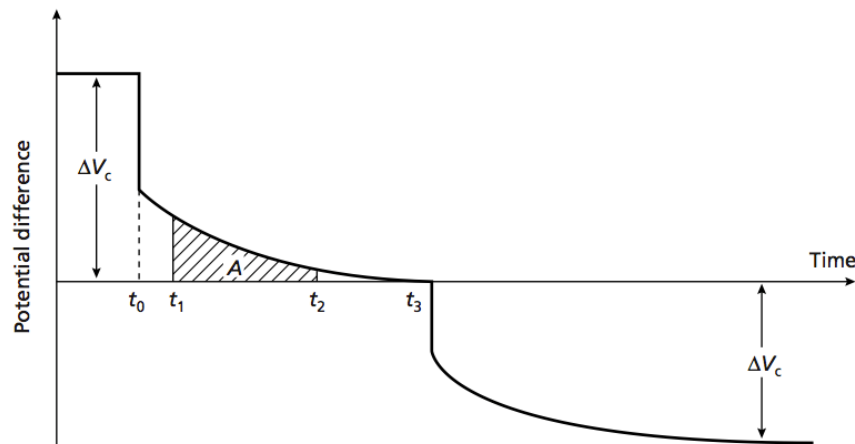


Figure 2.4 Induced Polarization exhibited on a plot of potential versus time. The area *A* is chargeability, one measure of the gradual decay in potential that results after the introduced current is abruptly shut off (Kearey et al., 2002).

The electrochemical mechanisms behind the IP phenomenon can also give insight into the subsurface rock composition, since high induced polarization primarily occurs in two situations. In the first instance, since rock-forming minerals generally develop a negative net charge on their surfaces, positive ions will collect in the adjacent pore fluid; if this collection of positive ions

extends into the pore fluid, on the order of the diameter of the pore itself, electrolytic flow will be blocked, causing a build-up in charge. This effect is known as Membrane Polarization, and is most often associated with the presence of clays and low salinity in the pore fluid (Figure 2.5a).

Alternatively, a pore may be blocked by a conductive metallic grain, which will also cause a build-up in charge on both sides of the grain (Figure 2.5b). This effect is known as Electrode Polarization, and can indicate the presence of a potential ore body. Due to the alluvial nature of the Cienega Creek study area, Membrane Polarization is the most likely source of any anomaly in IP.

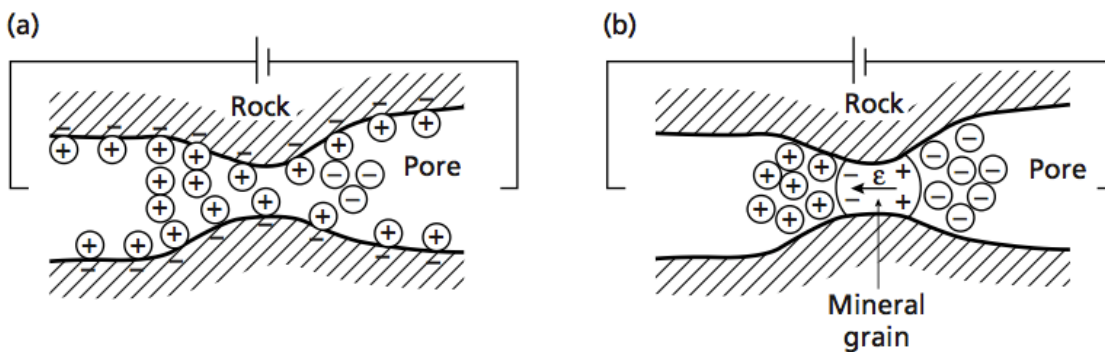


Figure 2.5 Induced Polarization mechanisms: (a) Membrane Polarization and (b) Electrode Polarization (Kearey et al., 2002).

2.4 Inversion

The relatively straightforward analytical processes used to derive apparent resistivities and IP values for each data point in a survey area are only suitable for simple geologic cases, such as homogeneous half-spaces. In order to create a more accurate representation of subsurface electrical properties, it is necessary to resort to computationally intensive numerical methods. The use of such methods to calculate a geologic solution for the observed resistivities is known as inversion.

While inversion is an extremely valuable tool for interpretation, it is important to remember its limitations. A good inversion model should correlate relatively well with the observed apparent resistivity pseudo-section, but inversion models often introduce suspect anomalies that are not evidenced in the observed data. One way of determining the quality of an inversion model is to use forward modeling to reverse the process and create a calculated apparent resistivity pseudo-section; if this calculated pseudo-section is a close match to the observed pseudo-section, then the inversion model is more credible.

3. DC Resistivity Surveys using Zonge International Instrumentation and Modeling

3.1 Introduction

Direct Current (DC) Resistivity surveys using Zonge International instrumentation was used to collect dipole-dipole complex resistivity data around the Empire Ranch Headquarters (HQ) and the Cieneguita Cienega Complex (Map 3.1). A GGT-3 geophysical transmitter and GDP-32²⁴ receiver were used to acquire apparent resistivity and phase angles (Zonge 2017). The results are displayed in cross-sections with the intent to locate potential clay layers and possibly depth to water table.

3.2 Electrical Resistivity Survey Location

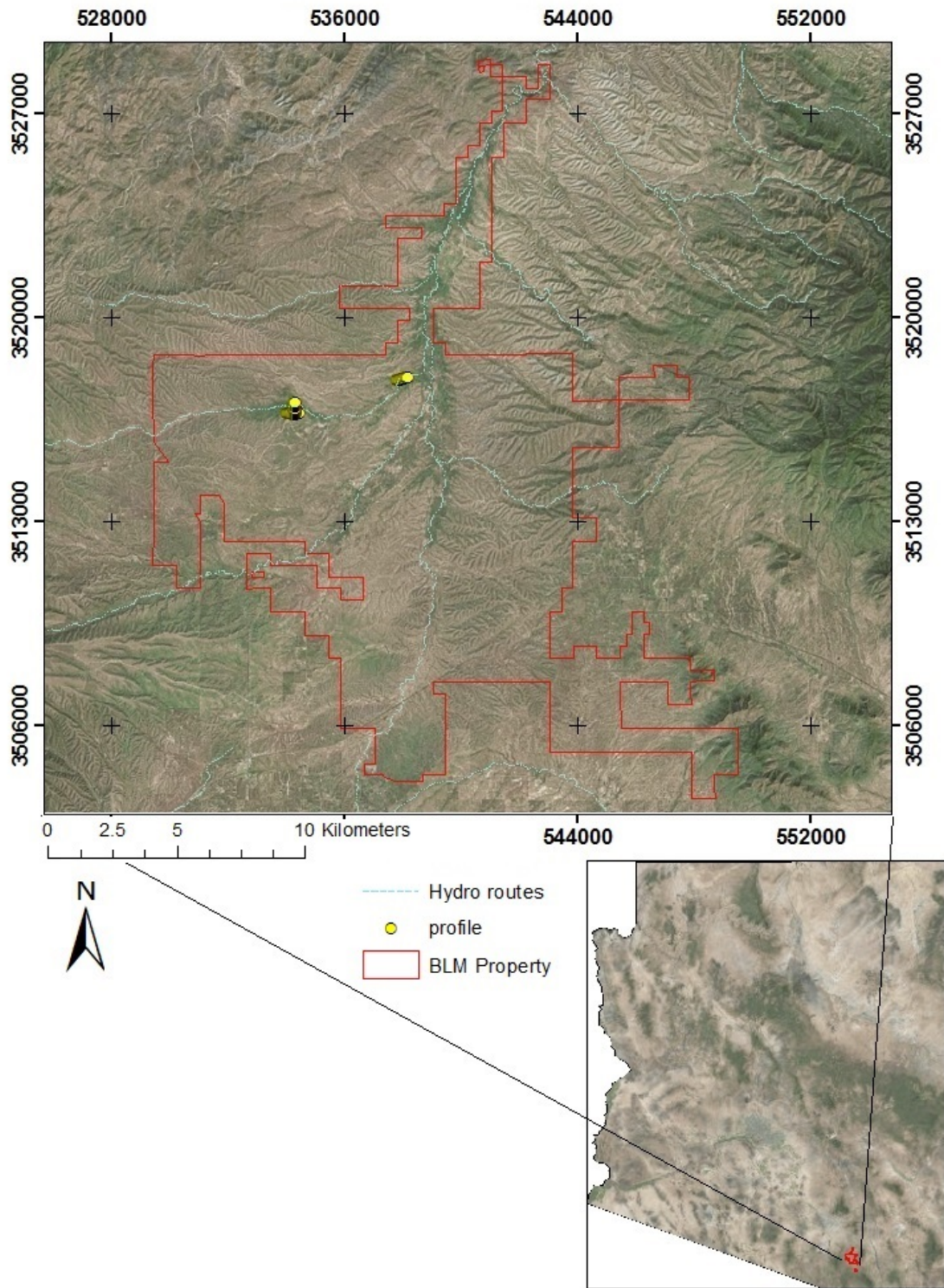
The Resistivity (RES) and Induced Polarization (IP) surveys used the GDP-32 for data collection. Receiver porous pots were placed at 50-meter intervals, with the transmitter line offset 10 meters. All efforts were made to avoid interference such as fences. The IP/RES survey lines are displayed on Maps 3.1, 3.2, and 3.3.

Lines Z1 and Z2 are east of Empire Ranch Headquarters with Line Z2 crossing Empire Gulch (Map 3.2). Line Z1 runs east to west and Line Z2 runs south to north. Line Z2 also crosses Line Z1, with the most southern transmitter approximately 30m S of Line Z1. Line Z3 is in Empire Wash northeast of Lines Z1 and Z2, west of Cienega Creek and in the Cieneguita Cienega Complex (Map 3.3). Line Z3 runs southwest to northeast between two fences. See Table 3.1 for UTM coordinates of exact location of the ends of the profiles.

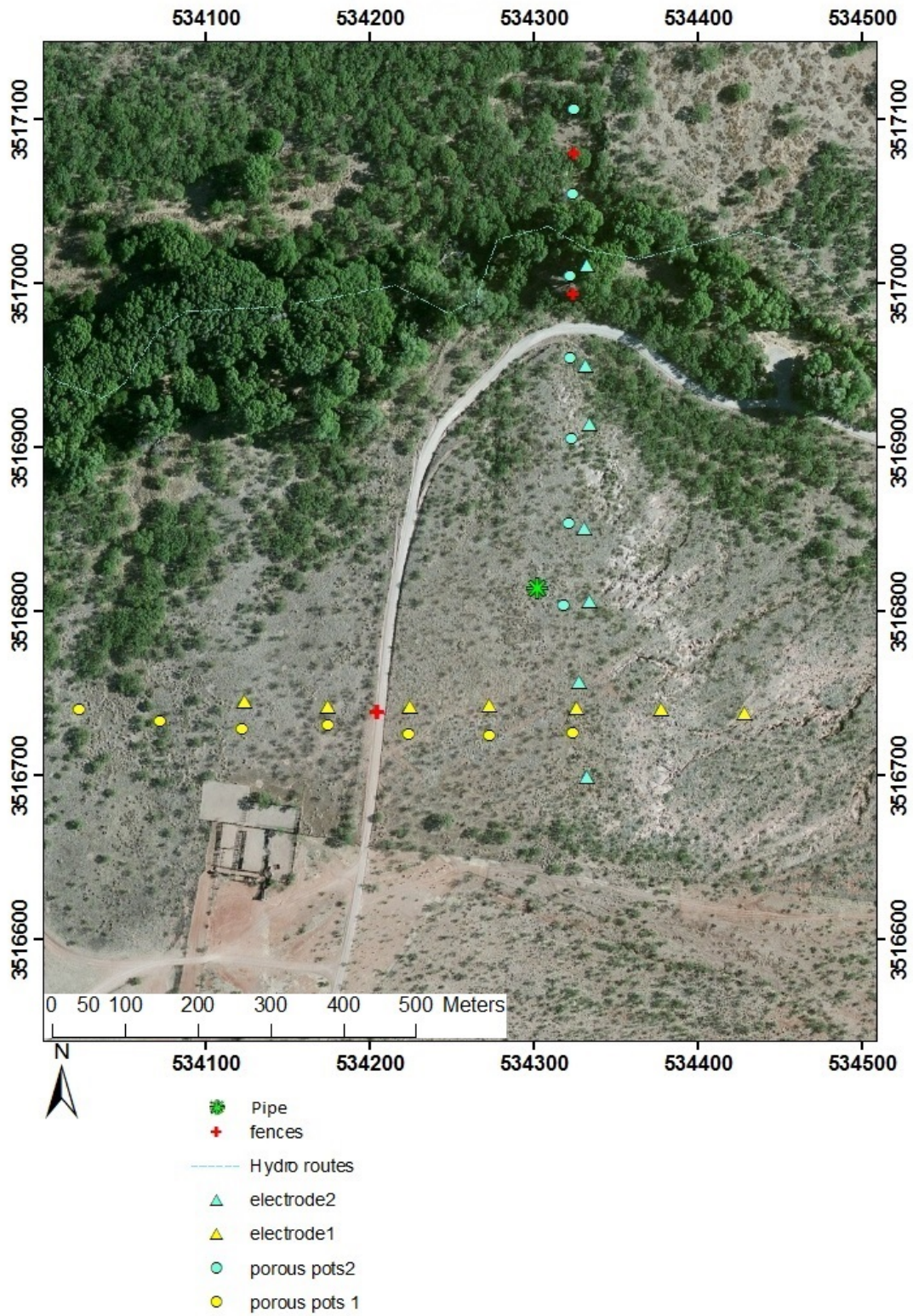
In order to avoid interference with the current paths, three fences were cut during the data collection and then repaired for Lines Z1 and Z2. A large pipe was also present above ground southeast of the road, but was roughly 20 meters from the lines and interference was not anticipated (Map 3.2). A 50-meter distance was maintained from the southern fence on Line Z3, but at one location, the northern barbed wire fence was 30 meters away from the transmitter line, on a ridge higher in elevation than the electrodes (Map 3.3).

Table 3.1

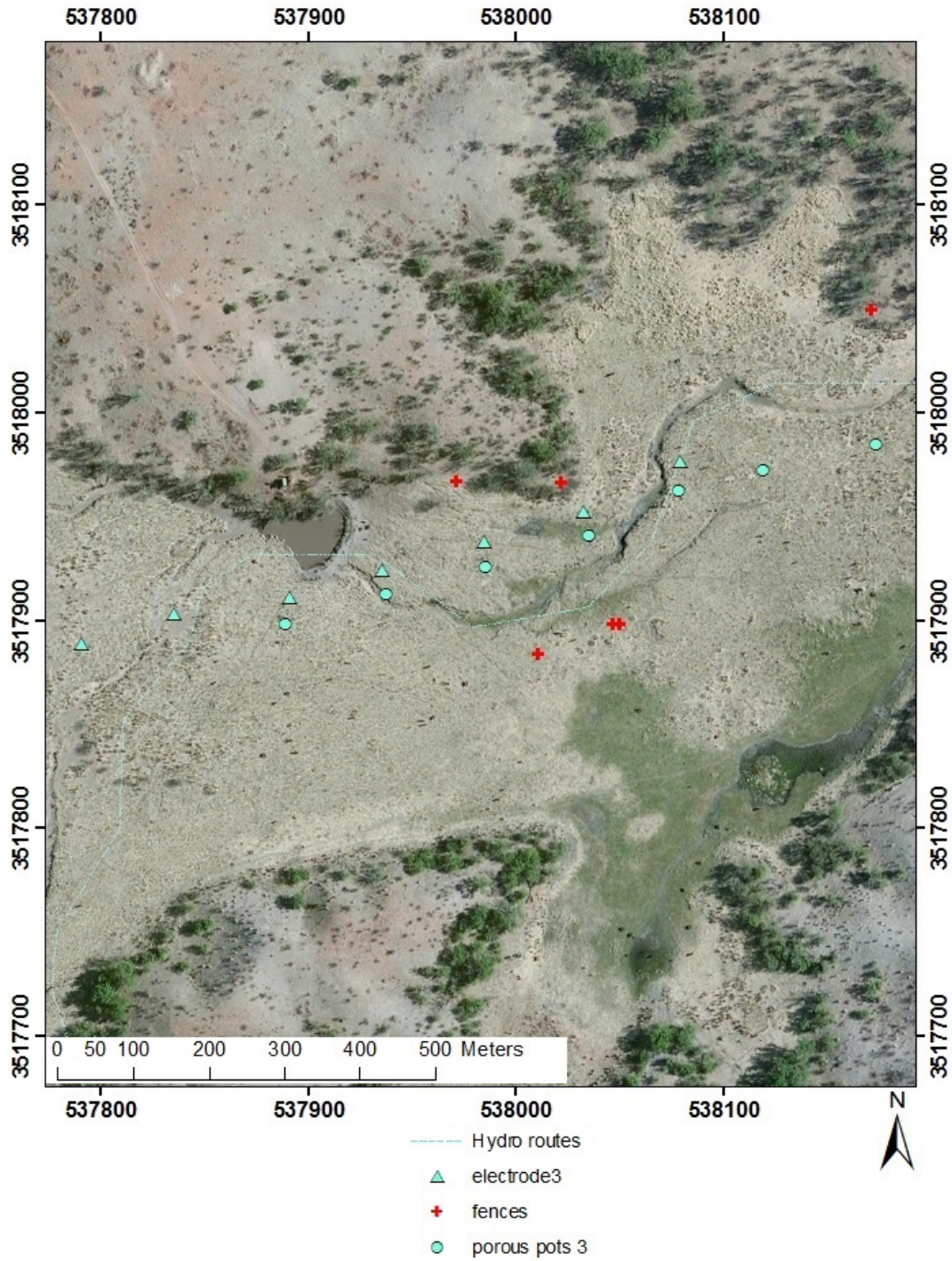
Description	Western transmitter	Eastern transmitter
Line Z1 W-E	534429E, 3516738N	534023E 3516741N
Description	Southern transmitter	Northern transmitter
Line Z2	534333E, 3516699N	534324E, 3517107N
Description	Western transmitter	Eastern transmitter
Line Z3	537791E, 3517889N	538173E, 3517985N



Map 3.1: Profile Locations.



Map 3.2: Profile Lines Z1 and Z2.



Map 3.3: Profile Line Z3.

3.3 Instrumentation and Field Procedures

Three lines of electrical resistivity and induced polarization data were collected using a Zonge GDP-32 multi-channel receiver (Figure 3.4). Two of the lines were oriented east-west and another was oriented north-south. The data were collected using a dipole-dipole array with an a-spacing of 50 meters. The array was set up using standard Zonge equipment: First, a 3kW ZMG-9A gas powered generator was connected to a ZPB-600 voltage regulator, which was used to regulate the voltage and output it to the GGT-3 transmitter unit (Figure 3.1 and 3.2). The transmitter unit was also connected to an XMT-32S transmitter controller unit, which kept the frequency at 1 Hz throughout the entire experiment (Figure 3.3).

This setup was placed near the midpoint of each line along with the GDP-32 receiver unit. The transmitter was connected to a series of transmitting electrodes, each comprised of five metal stakes driven into the ground at each location, soaked in water, and connected in parallel to lower the contact resistance with the earth. The GDP-32 was connected to a series of copper sulfate porous pot receivers, which were buried at each station and soaked in water to reduce the contact resistance between the receiver and the earth. These transmitter and receiver lines were parallel and offset by approximately 10 meters in order to prevent the wires connected to each electrode from creating electromagnetic coupling with each other, which would add interference to the collected data.

The array of receiver electrodes was 400 meters long for each line. An estimate of the depth of investigation for this array is $0.2 * \text{the array length} = 80 \text{ meters}$. The transmitter and receiver lines were also shifted inline by 100 meters, so that the transmitter line extended by two transmitters on one end while the receiver line extended by two extra receivers on the other (Figure 3.7 a-c). The logic behind this geometry is while the system is operational there is a 50m spacing between the 'live' transmitters and the nearby receivers (Figure 3.7a). Therefore as the transmitters are turned on and off along the line the receivers near the live transmitters are being turned off (Figure 3.7 a-c). This geometry reduces interference in the collection and collects the most data from the 300m line of receivers. This does not result in any data loss, however, since keeping these transmitters in the array would only result in redundant data collection (Figure 3.7c).



Figure 3.1. 3kW ZMG-9A gas powered generator.



Figure 3.2. Zonge GGT-3 Transmitter.



Figure 3.3. XMT-32S Transmitter Controller.



Figure 3.4. Zonge GDP-3224 Multi-Function Receiver.



Figure 3.5. Porous pot receiver electrode.



Figure 3.6. Pentagon of metal stakes used as a transmitting electrode.

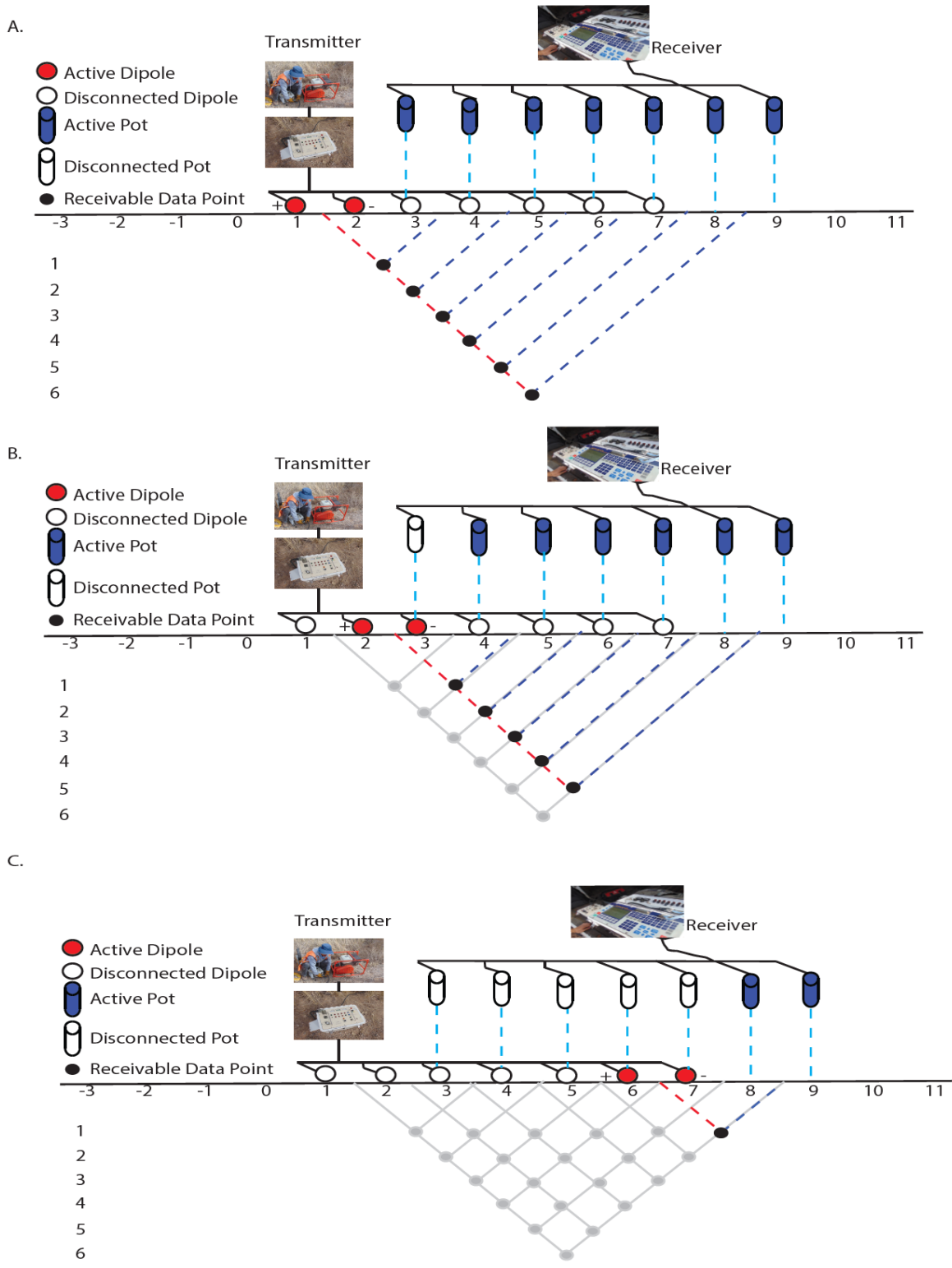


Figure 3.7a-c. Zonge International Diagram of the dipole-dipole array. (Source: Zonge International Co.).

3.4 Results

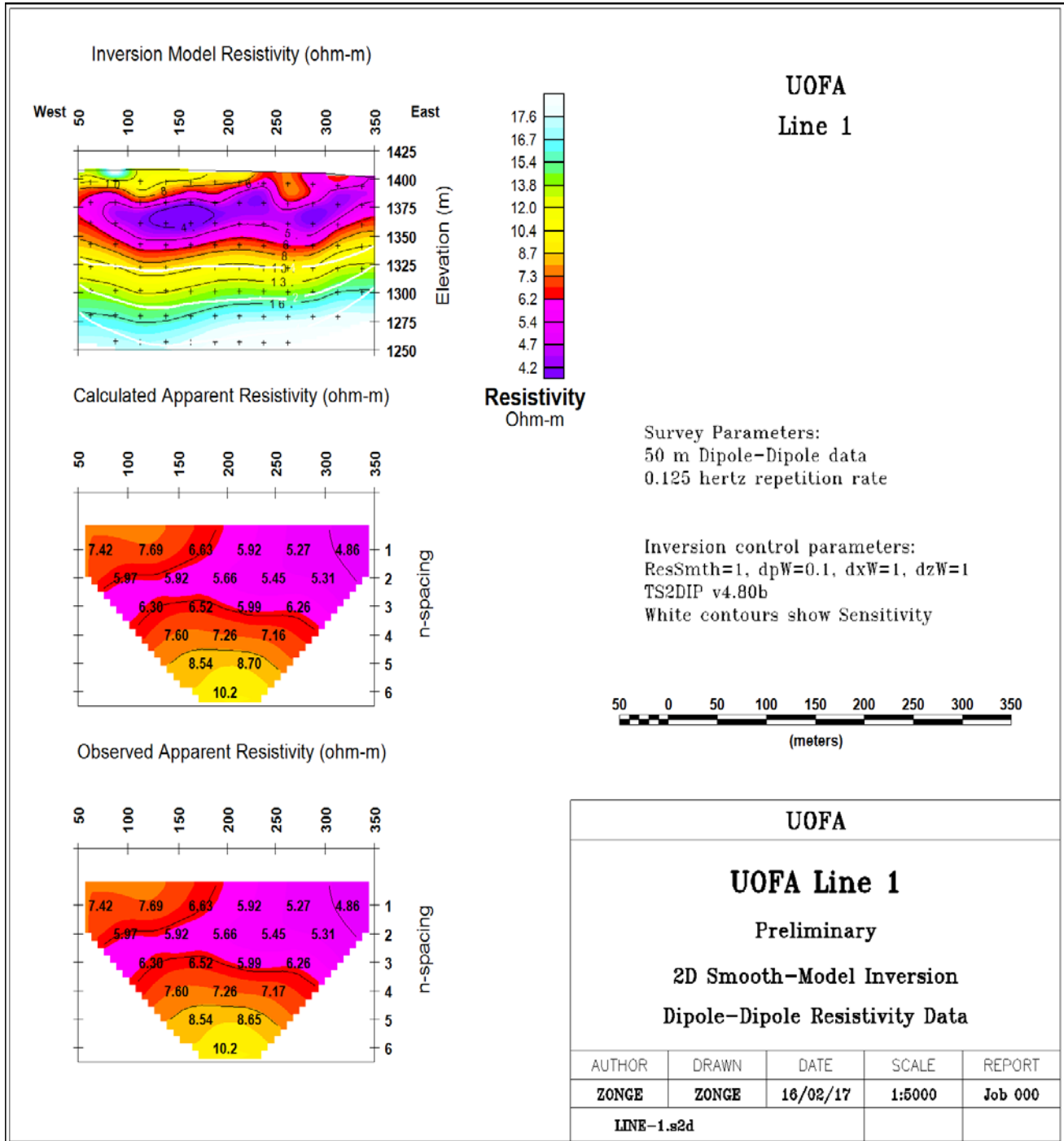


Figure 3.8. Line Z1 electrical resistivity inversion. This image contains the apparent resistivity, the inverted resistivity model, and the calculated resistivity based on the model. The observed and the calculated apparent resistivities are almost identical, indicating that the model produced a solution that is a very good fit. Note that the repetition rate was actually 1 Hz, not 0.125 Hz.

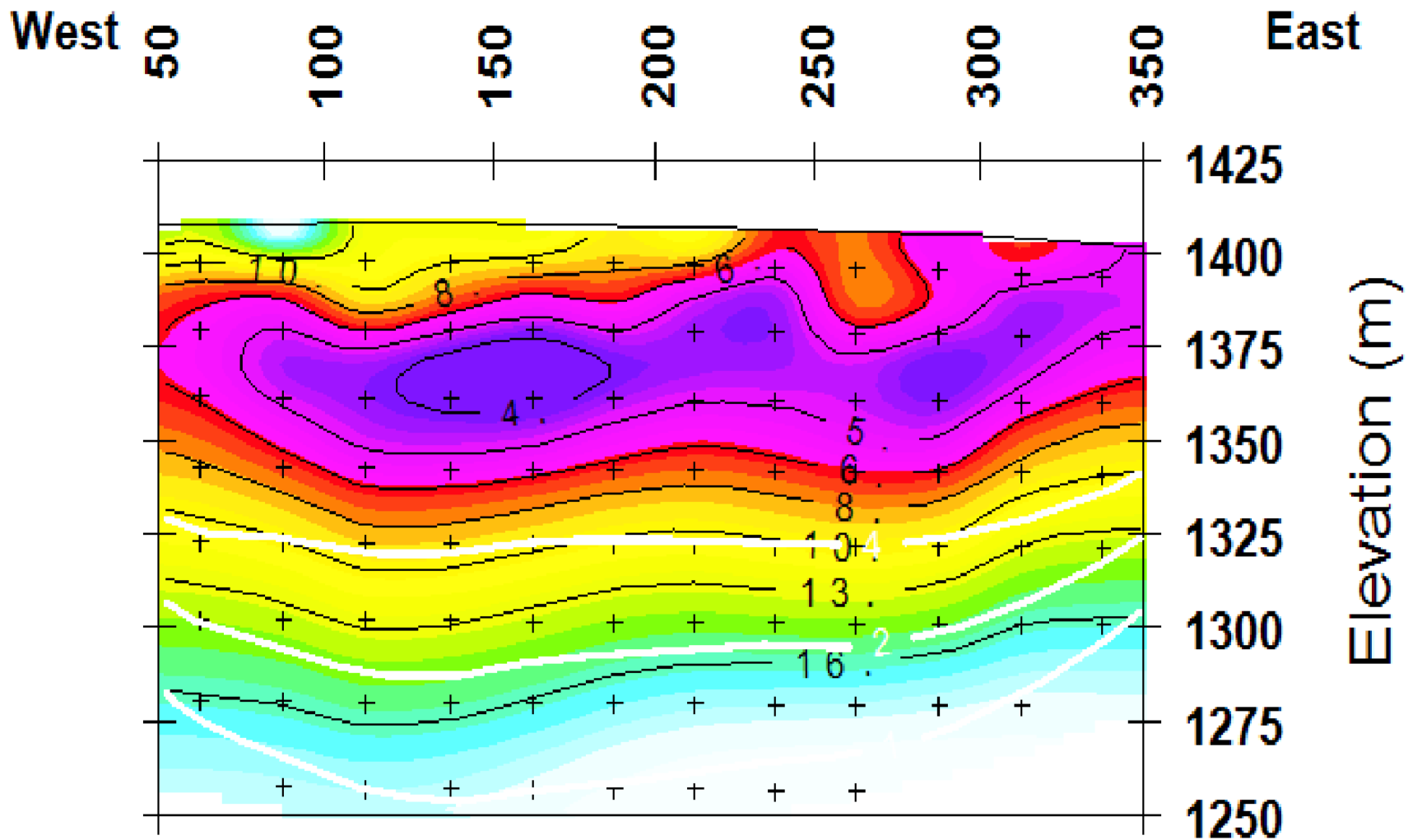


Figure 3.9. LineZ1 Inversion Model Resistivity.

The resistivity model from Line Z1 (Figure 3.9) shows a series of sub-horizontal bands of increasing resistivity with depth, as well as a patch of higher resistivity near the beginning of the line. This may indicate that there is water just beneath the surface, perhaps bounded by a lower porosity unit, which could be indicated by the higher resistivity yellow and green bands. The eastern portion of this line connects to the southern edge of Line Z2, and the data in both of these locations are quite similar. This indicates that the data collection was consistent across both lines and that the resistivity in this area is homogeneous.

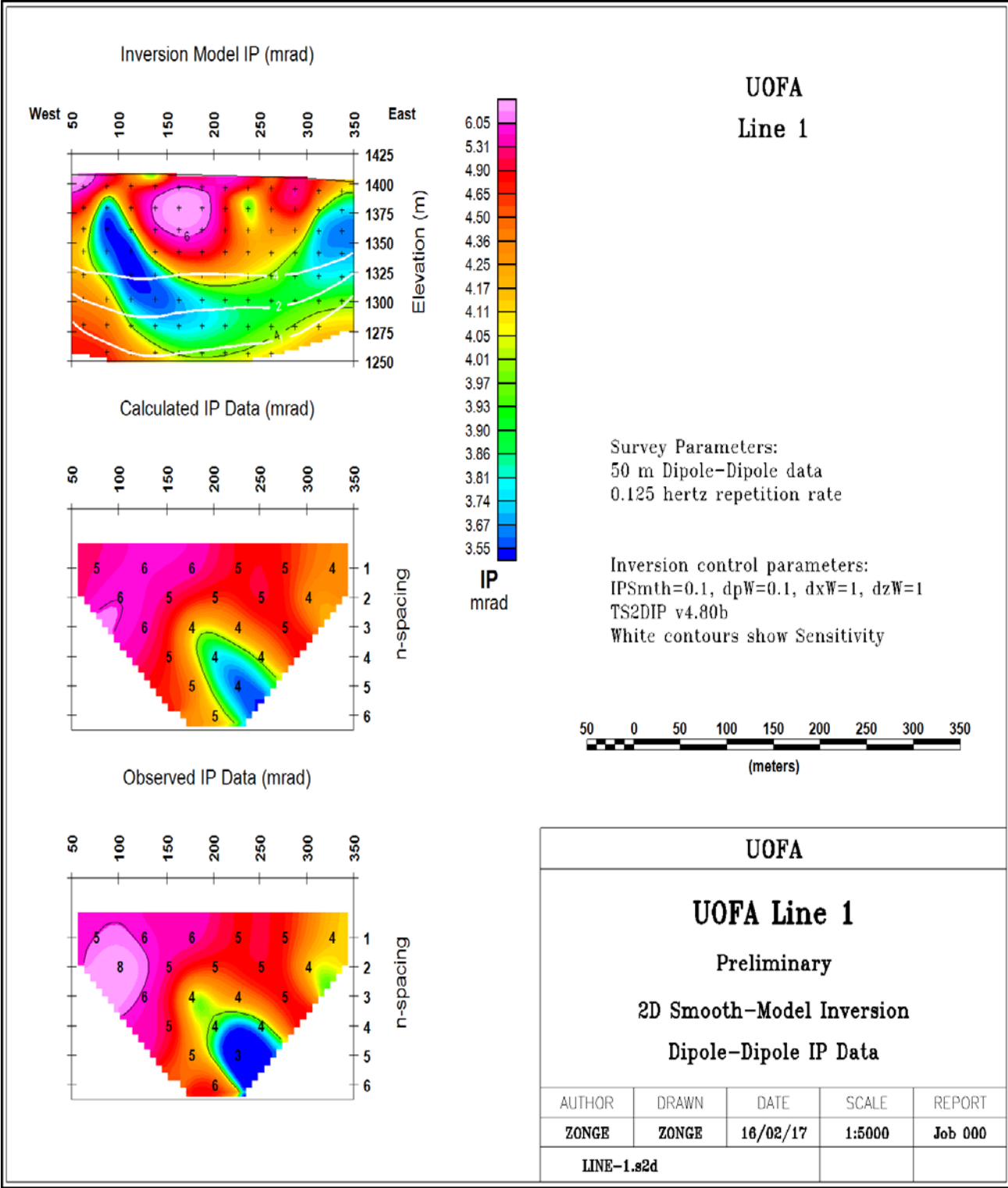


Figure 3.10. Line Z1 induced polarization inversion. This image includes observed, calculated, and inverted IP data. The calculated and observed data are very similar indicating the inverted model is a good fit. Note that the repetition rate was actually 1 Hz, not 0.125 Hz.

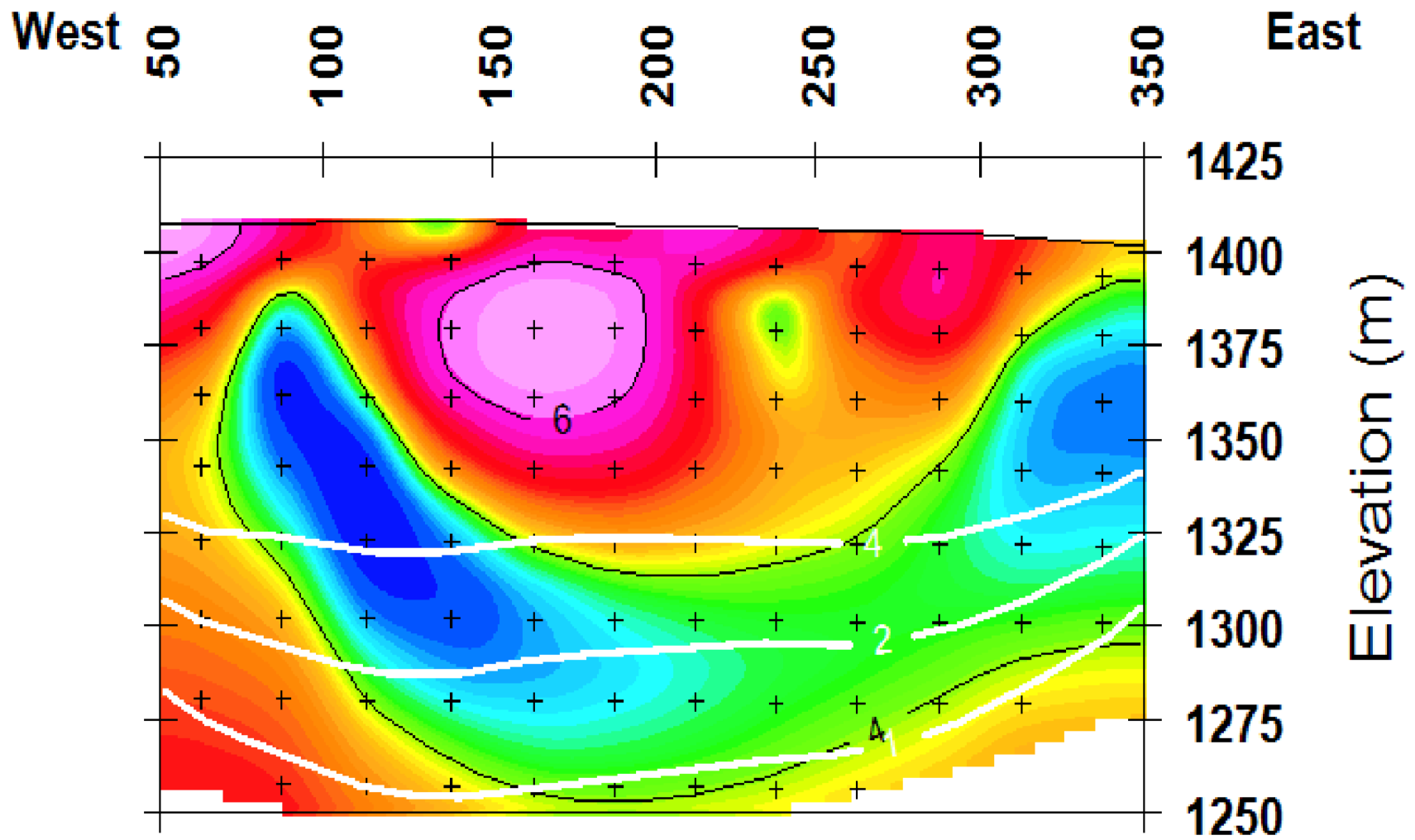


Figure 3.11. Line Z1 Inversion Model.

At Las Cienegas, higher IP readings may be associated with clays. In this case, it seems as though there are clays near the surface, which matches the low resistivity layer seen in Figure 3.11. The lower IP zone just beneath this could be a non-porous, non-mineralized rock layer, which would create a resistive, non-chargeable zone. The eastern edge of this data is also shared with the southern edge of Line Z2. The two models don't quite match at this location however, indicating that either the earth properties are inhomogeneous or there were differences in data modelling.

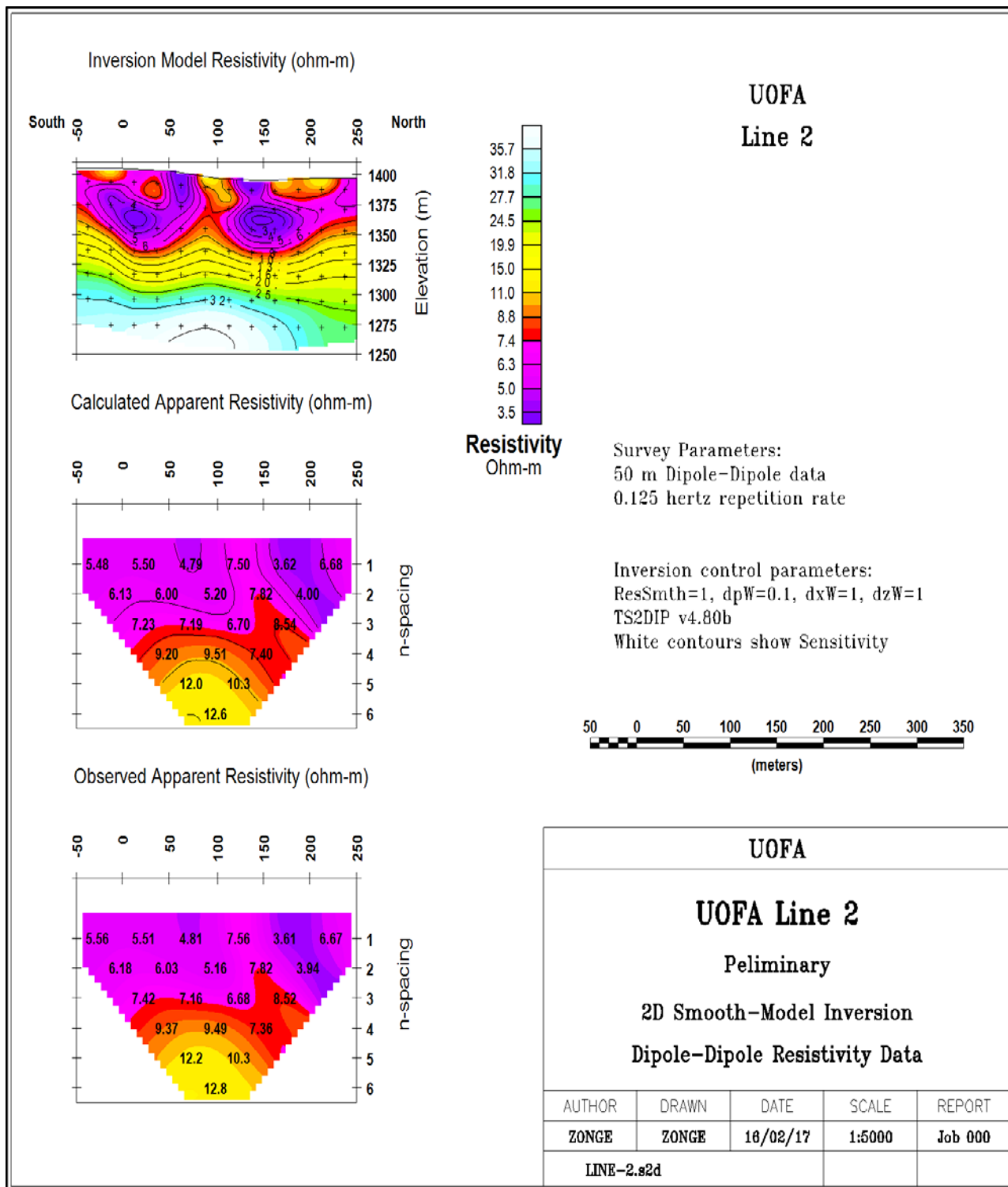


Figure 3.12. Line Z2 electrical resistivity inversion. This image contains the inverted resistivity model, apparent and calculated resistivity based on the model. The observed and the calculated apparent resistivities are nearly identical, identical, indicating a good fit. Note that the repetition rate was actually 1 Hz, not 0.125 Hz.

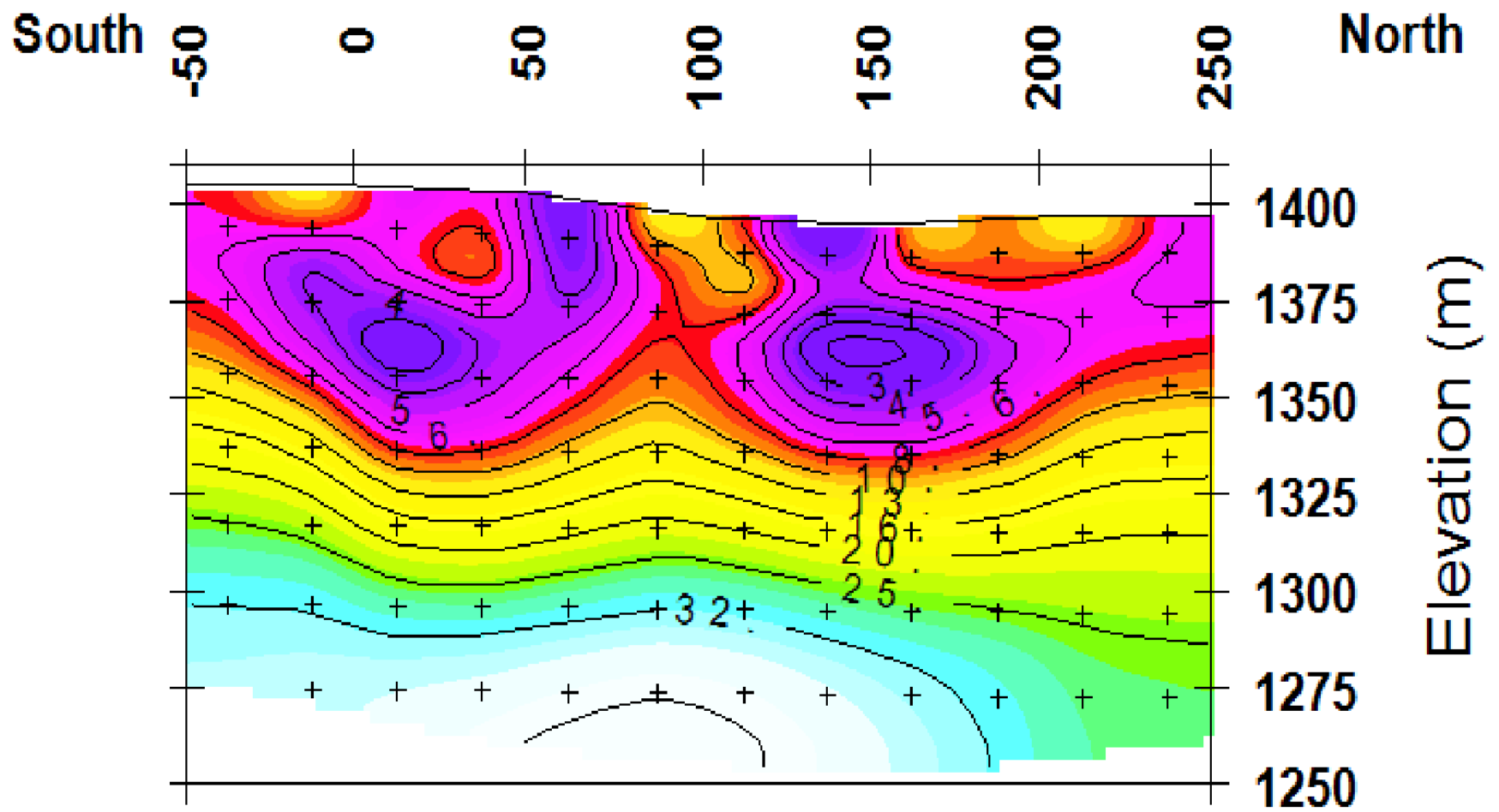


Figure 3.13. Line Z2 Inversion Model Resistivity.

The resistivity model for Line Z2 (Figure 3.13) resembles that of Line Z1, with an asymmetrical band of low resistivity near the surface overlaying layers of progressively higher resistivity. Three prominent pockets of higher resistivity also exist at the surface. The low resistivity band could indicate a layer of clay or water saturated soil, while high resistivity pockets could be lower porosity rock units.

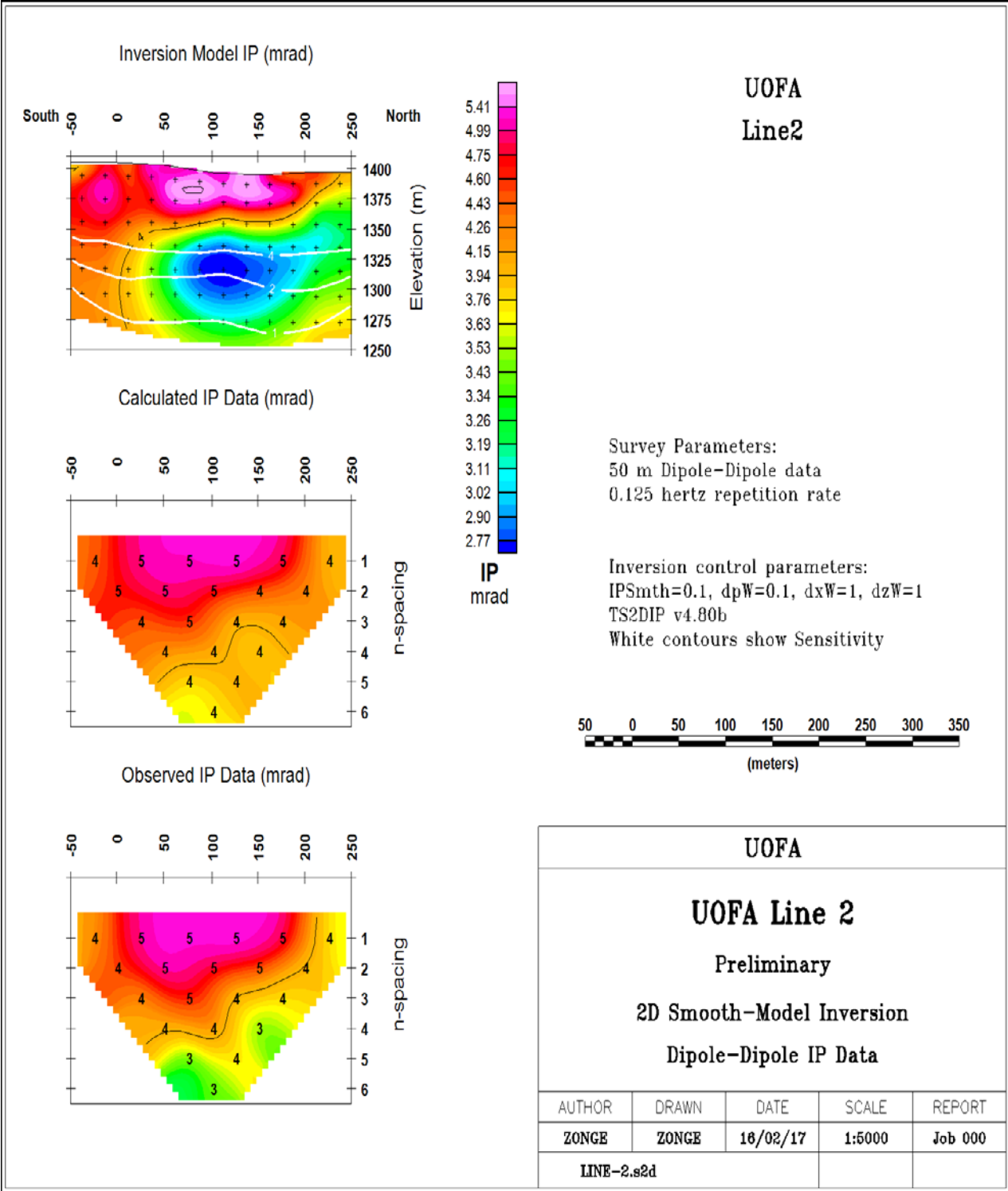


Figure 3.14. Line Z2 induced polarization inversion. This image includes observed, calculated and inverted IP data. The calculated and observed data are very similar, indicating that the inverted model is a good fit. Note that the repetition rate was actually 1 Hz, not 0.125 Hz.

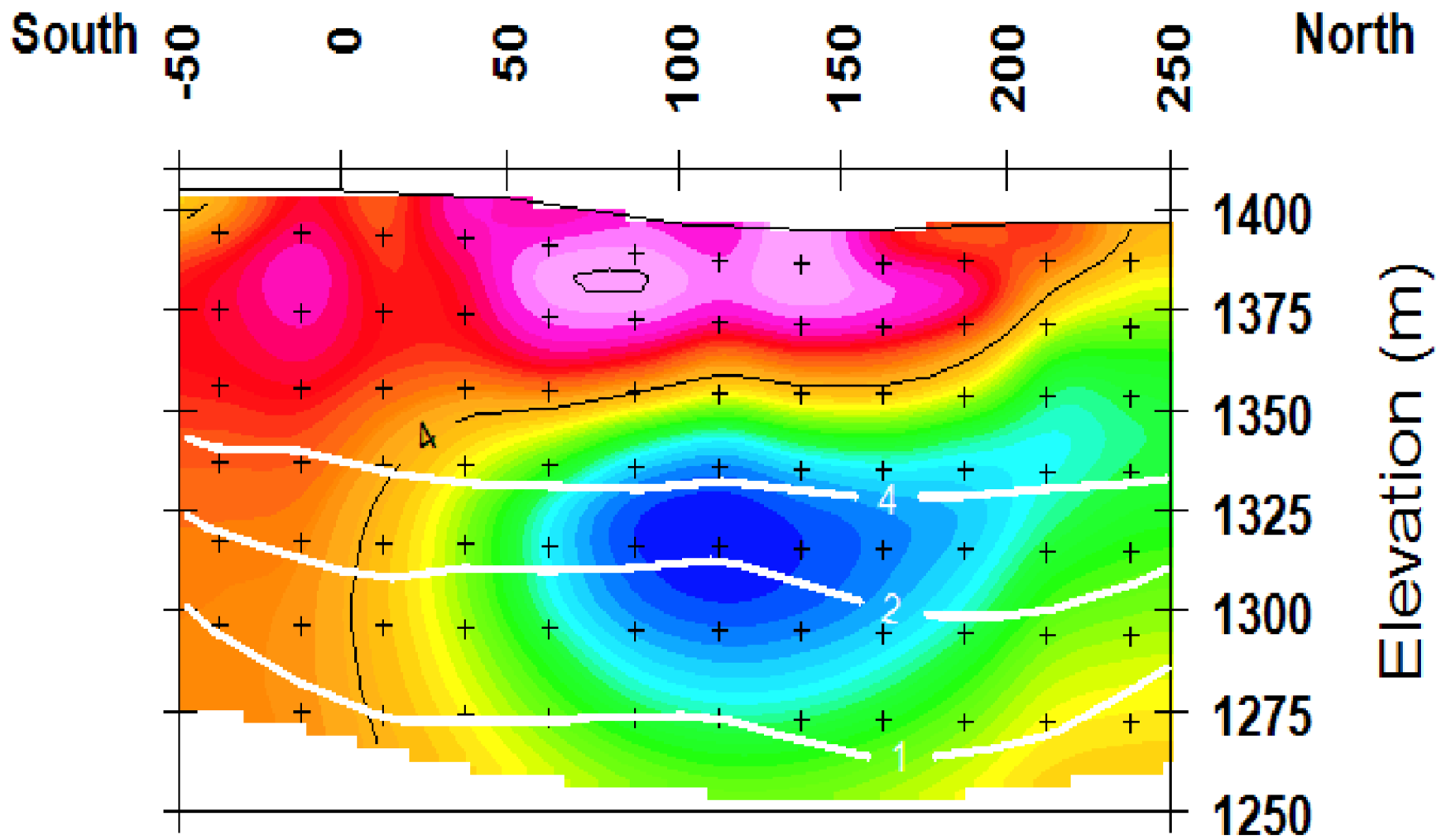


Figure 3.15. Line Z2 Inversion Model IP.

At Las Cienegas, higher IP is indicative of clays. This implies that there may be clays near the surface along line 2 (Figure 3.15), which is corroborated by the low-values in the resistivity data. The low IP zone beneath could represent a non-porous, non-mineralized rock layer, which would create a resistive, non-chargeable zone.

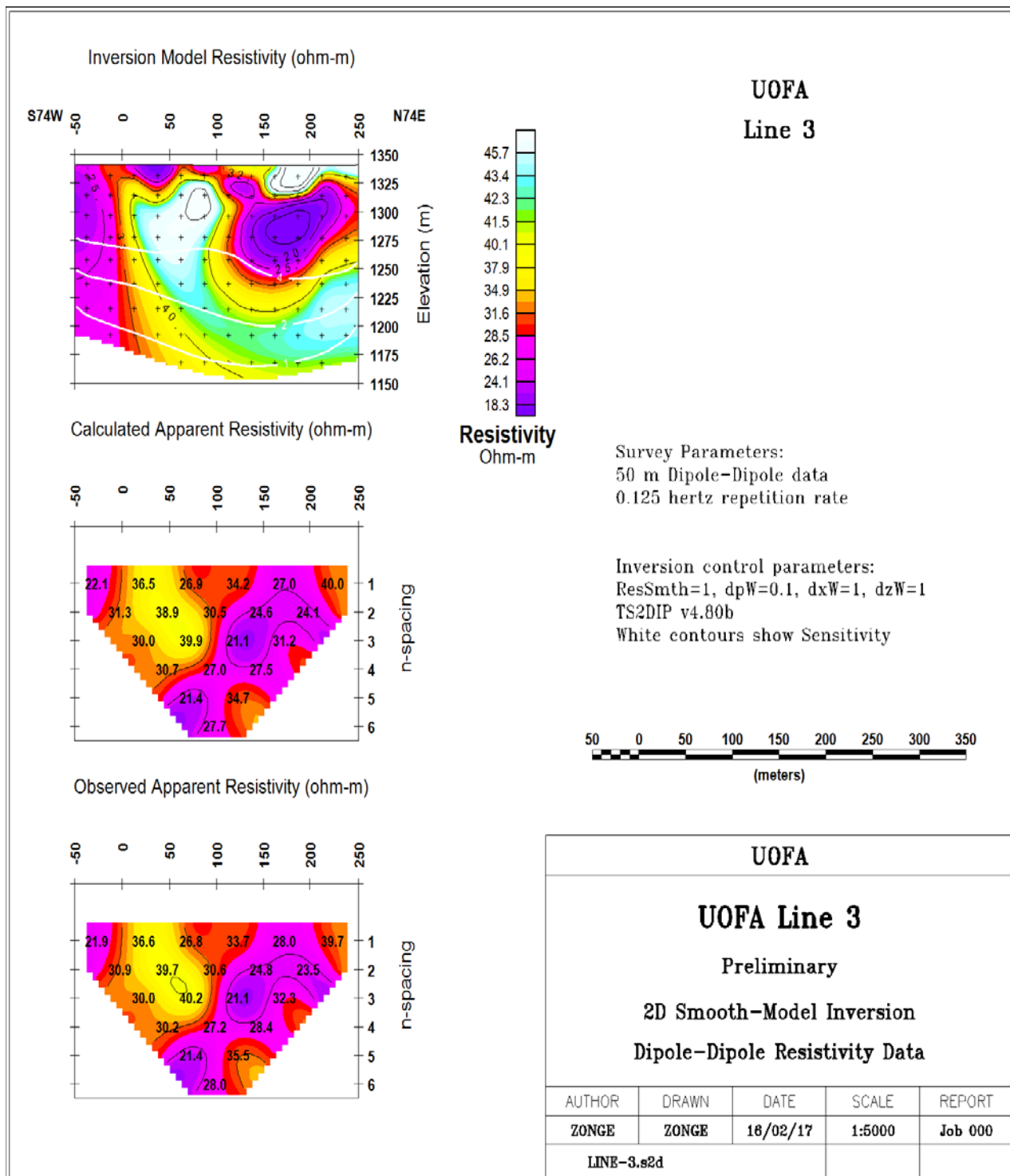


Figure 3.16. Line Z3 electrical resistivity inversion. This image contains the apparent resistivity, the inverted resistivity model, and the calculated resistivity based on the model. The observed and the calculated apparent resistivities are nearly identical, indicating a good fit. Note that the repetition rate was actually 1 Hz, not 0.125 Hz.

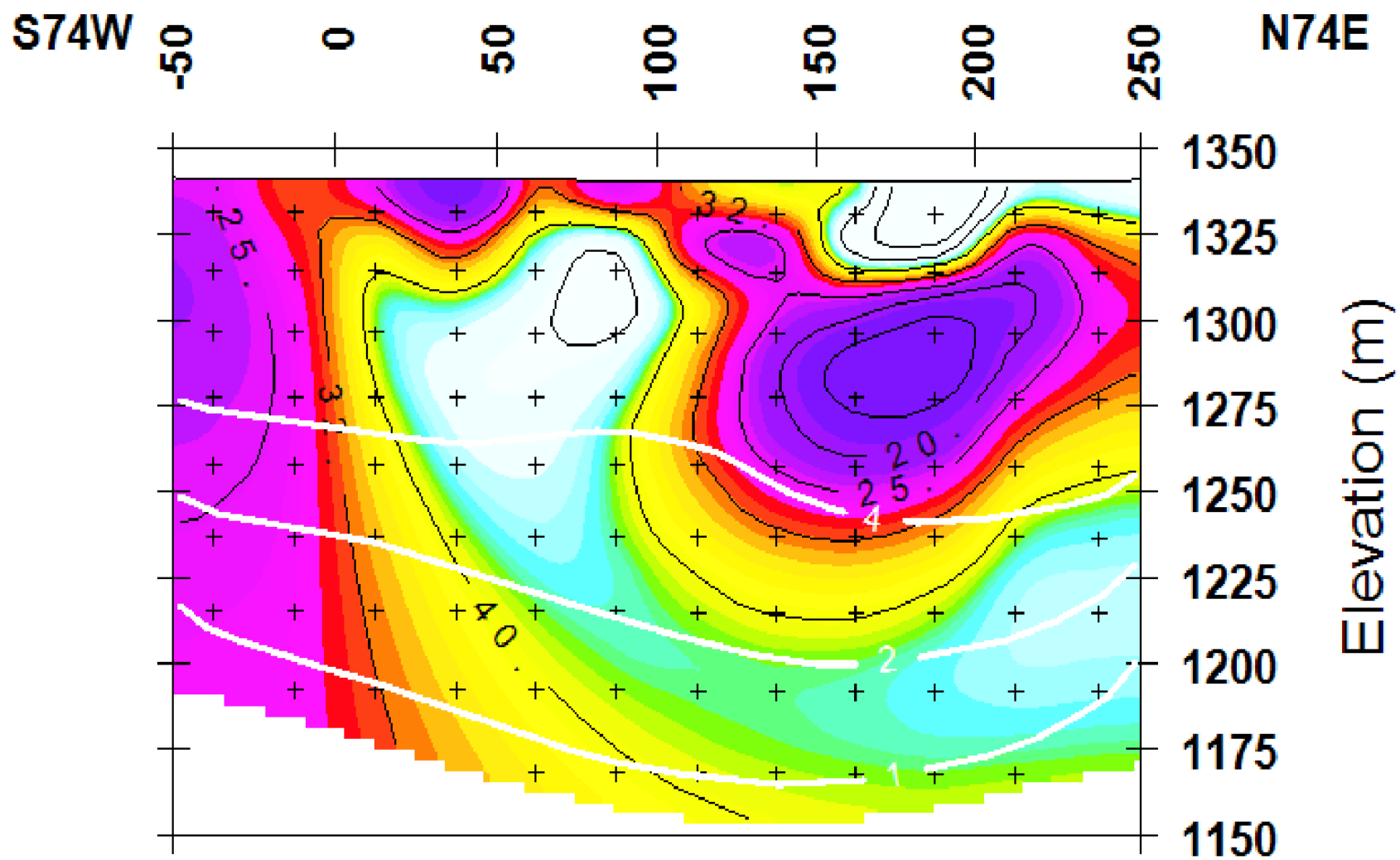


Figure 3.17: Line Z3 Inversion Model Resistivity.

The resistivity model (Fig. 3.17) from Line Z3, which crosses a small cienaga twice, shows significant variation along the profile line. Two regions of low resistivity exist, one at the surface on the far western end and another below the surface near the eastern end of the profile line. The low resistivity units may represent water-saturated clays, while the higher resistivity units may represent more compact clays.

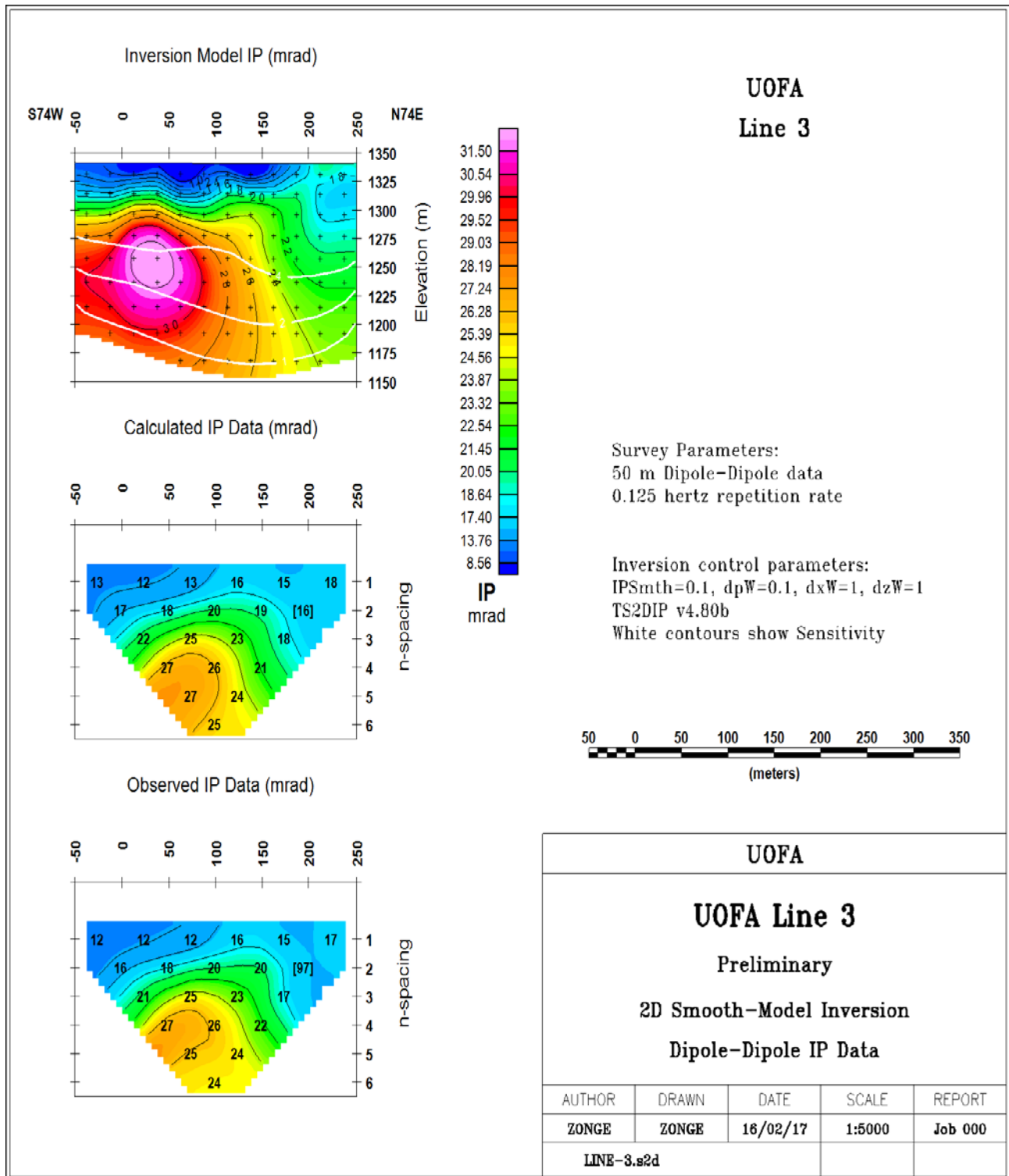


Figure 3.18. Line 3 induced polarization inversion. This image includes observed, calculated, and inverted IP data. The calculated and observed data are very similar, indicating that the inverted model is a good fit. Note that the repetition rate was actually 1 Hz, not 0.125 Hz.

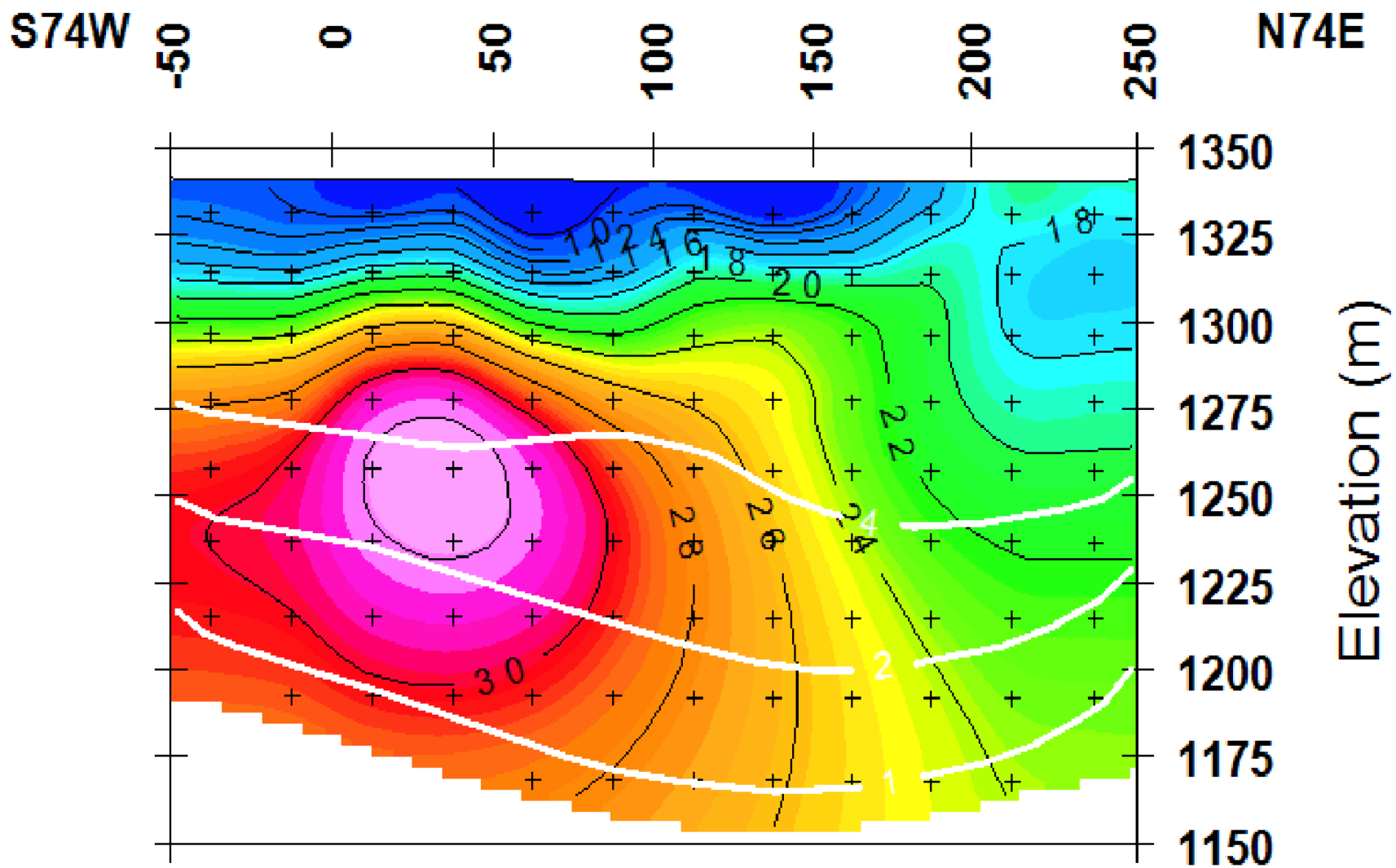


Figure 3.19. Line 3 Inversion Model IP.

For Line Z3 (Fig 3.19), high IP below the surface on the western end of the profile line indicates that clays may be present. The low polarization at the surface implies the presence of non-mineralized soils.

4. DC Resistivity Surveys using Hydrogeophysics, Inc. Instrumentation and Modeling

4.1 Introduction

The DC Resistivity survey using the equipment provided by Hydrogeophysics, Inc., was used to collect resistivity data around the Empire Ranch Headquarters (HQ) and the Cieneguita Cienega complex, in all but one case using an alternatively designed Wenner array (Map 4.1). One line, H0, was conducted using a Schlumberger configuration due to time constraints on field activities. Two lines were repeats of Zonge data previously collected, in order to compare the two different instruments (H5 and H8). The equipment used was a SuperSting R8 unit, but we used only apparent resistivity data. The results were modeled and all eight plots are displayed in Section 4.4.

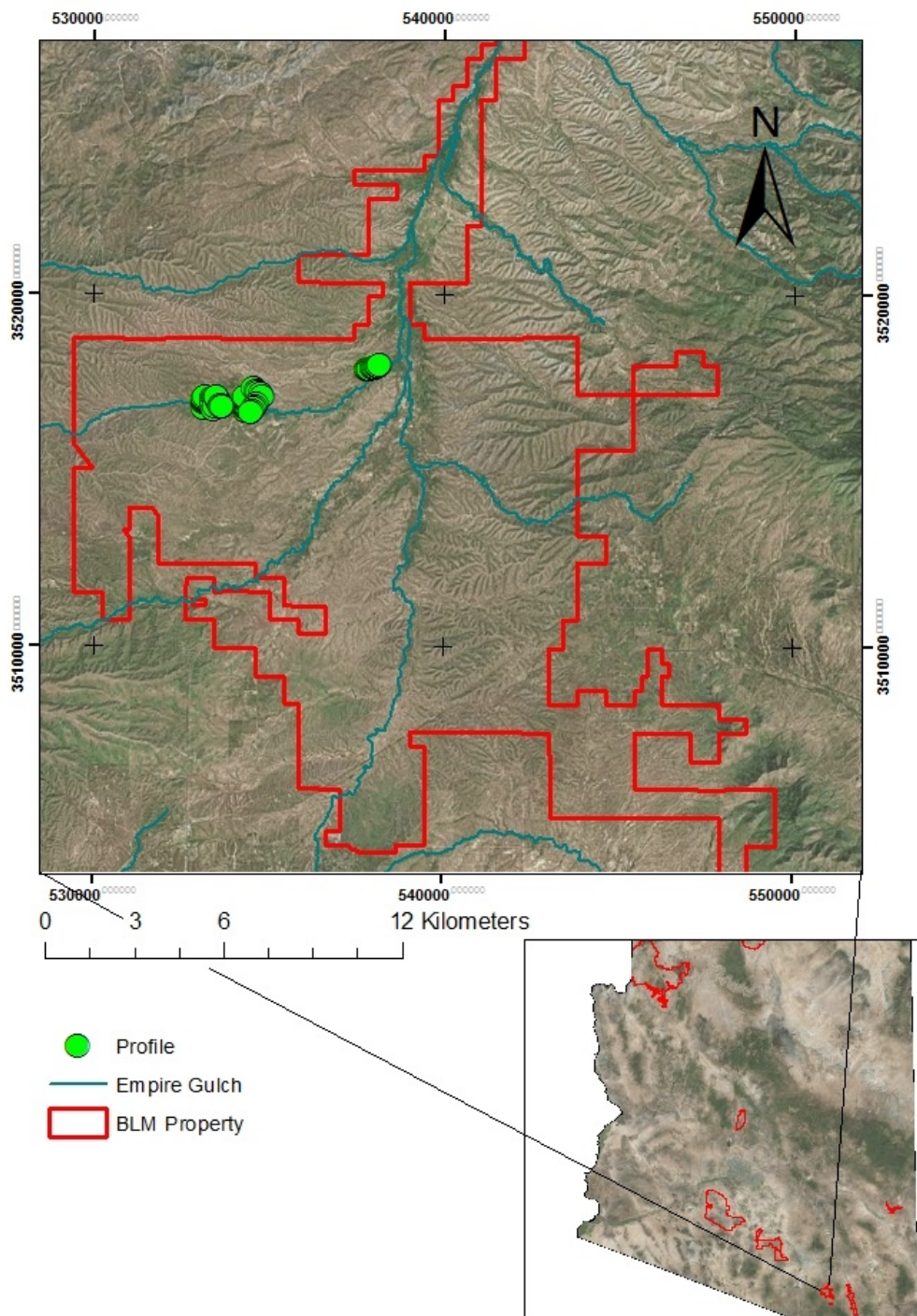
4.2 Electrical Resistivity Survey Location

Instead of individual transmitting and receiving lines or stations, the SuperSting utilized a long cable with takeouts every six meters for electrodes. The spacing between each of the electrodes was a constant 6 meters, and while efforts were made to avoid possible sources of interference, such as fences, the type of arrays used with this equipment allowed the lines to pass through fences and similar features with relatively little effect on the data.

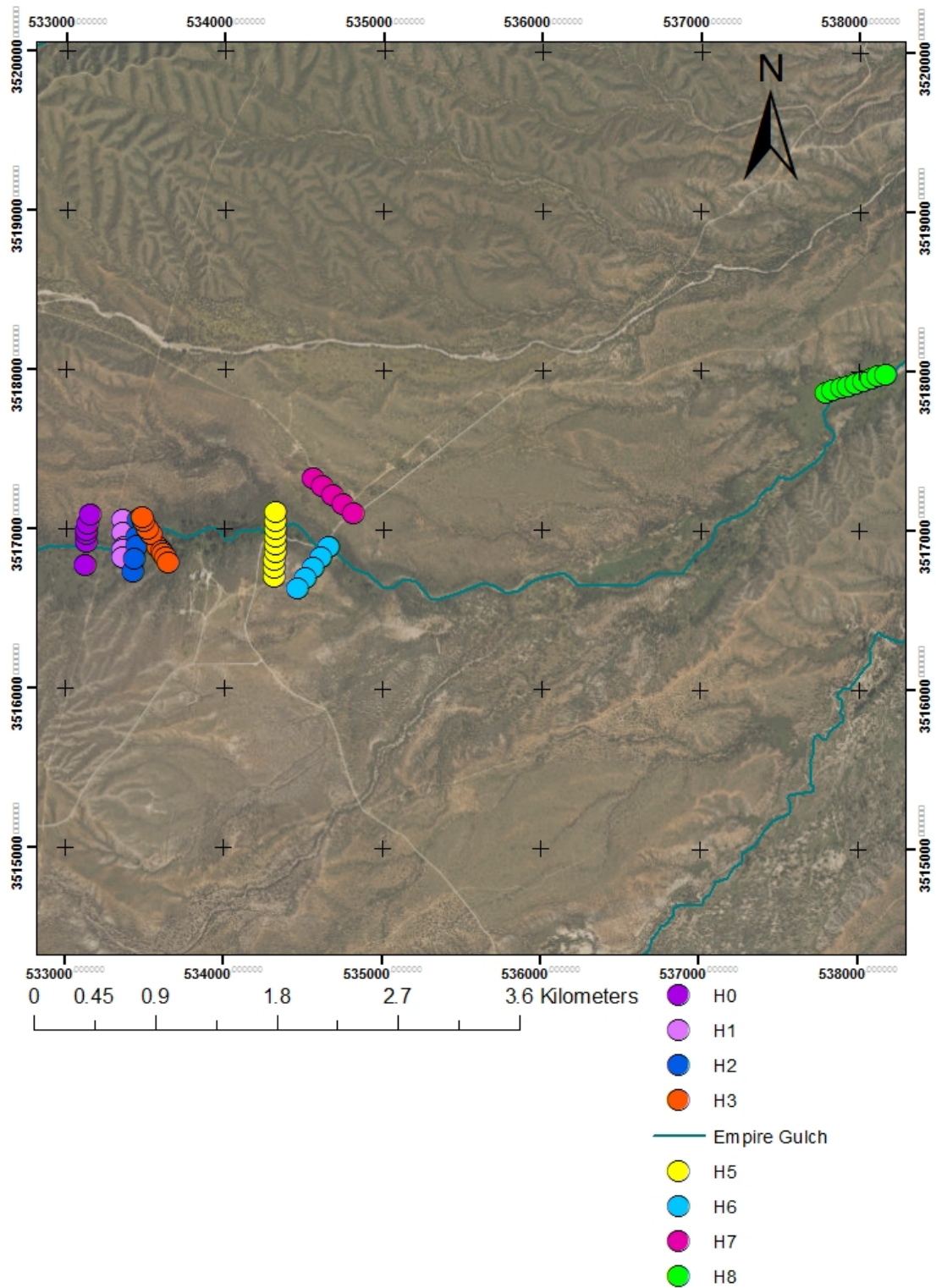
The surveys were bounded by line H0 on the west and line H8 on the east (Map 4.2). There was no line named H4. Lines H0, H1, H2, and H3 ran southwest to northeast across Empire Gulch (Map 4.3). Line H5 ran south to north across Empire Gulch, the same site as Zonge profile 2 (Map 4.4). Line H6 ran southwest to northeast across Empire Gulch (Map 4.4). Line H7 was north of H6, and ran southwest to northeast (Map 4.4). Line H8 ran southwest to northeast in the Empire Wash, the same site as Zonge profile 3 (Map 4.5). See Table 4.1 for UTM coordinates of exact locations of line beginnings and ends.

Table 4.1

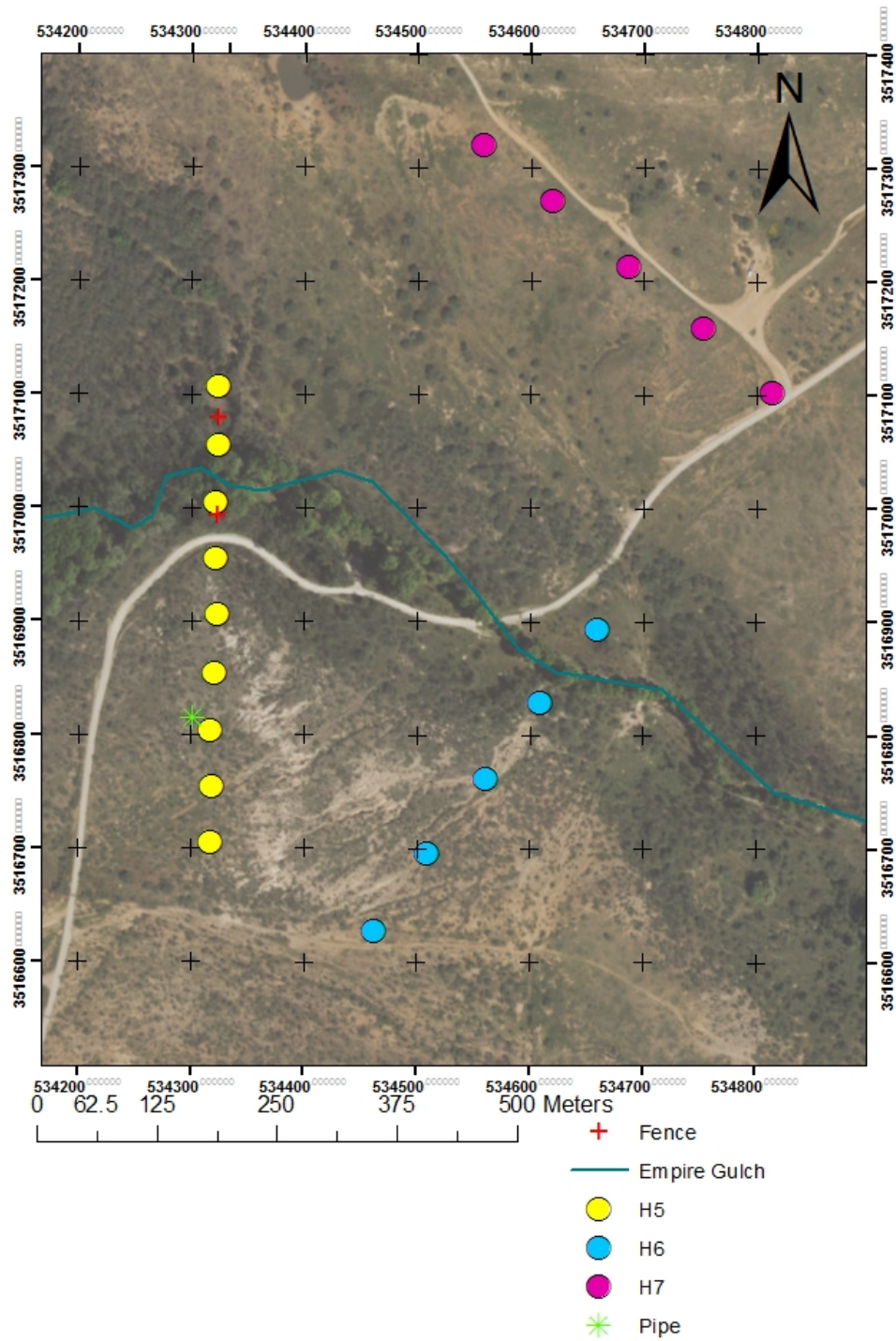
Profile Label	Line Beginning	Line End
H0	533120E, 3516772N	533156E, 3517091N
H1	533360E, 3516822N	533359E, 3517058N
H2	533428E, 3516730N	533462E, 3517059N
H3	533644E, 3516791N	533484E, 3517072N
H5	534333E, 3516699N	534324E, 3517107N
H6	534660E, 3516894N	534463E, 3516627N
H7	534814E, 3517103N	534558E, 3517320N
H8	537791E, 3517889N	538173E, 3517985N



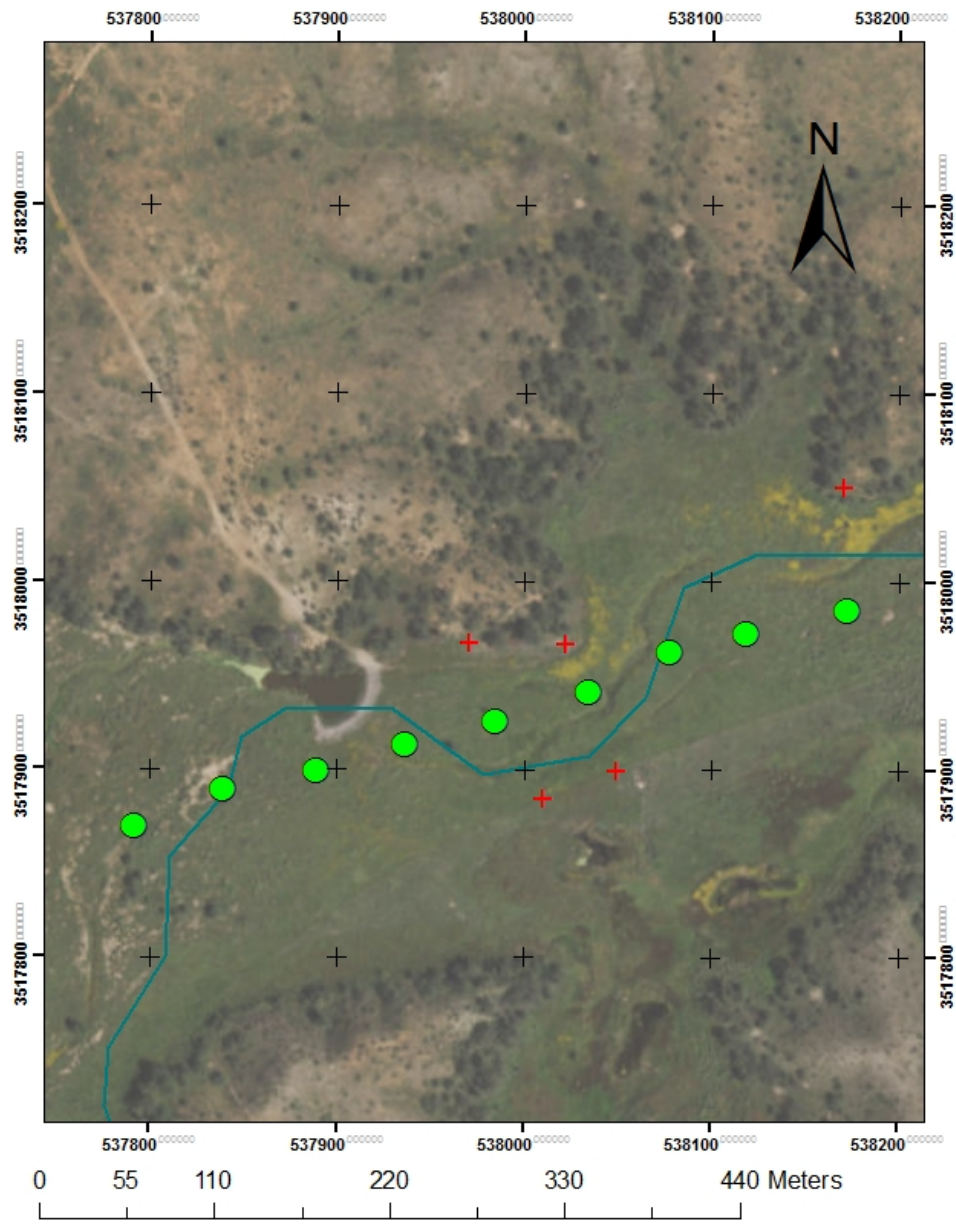
Map 4.1. Area of Interest.



Map 4.2, Lines H0, H1, H2, H3, H5, H6, H7, and H8.



Map 4.4. Lines H5, H6 and H7.



- + Fence
- Empire Gulch
- H8

Map 4.5. Line H8.

4.3 Instrumentation and Field Procedures:

The transmitter and receiver were contained in a single unit (SuperSting R8 unit, Figure 4.1b) which was powered by a battery source instead of a motor-generator. The console was connected to long power cables (Figure 4.1a) which had takeouts for metal stake electrodes.



Figure 4.1a. Transmitter/receiver cables had takeouts every 6 meters. These takeouts were connected to electrodes with the copper clips, also shown in this photo. These arrays were used to collect all of the information for the Schlumberger and alternative Wenner arrays.



Figure 4.1b. SuperSting control unit. Using a pre-created command file, this unit controls which electrodes are being used as transmitters and which are being used as receivers. This console also collects and stores all of the data collected in each line. This console is battery powered, and for this project standard car batteries were used. (Source: hgiworld.com)

A modified version of a Wenner array was used for the majority of these lines. The only exception to this was line H0, which was collected with a Schlumberger array to save time on data collection on that particular day. The Wenner array configuration can be considered a special case of the Schlumberger array: in each array, a pair of transmitting electrodes are on the outside of pairs of receiving electrodes. But in the case of a Wenner array, the distance between the transmitting electrode and the receiving electrodes is the same as the distance between the two receiving electrodes. In a Schlumberger array, this is not necessarily the case, and because of the variable distances the apparent resistivity calculations are slightly more complex. The modified Wenner array used in this project was the Alt_3 Wenner Array taken from Cubbage et al. 2017, seen below in comparison with the other resistivity arrays in Figure 4.2.

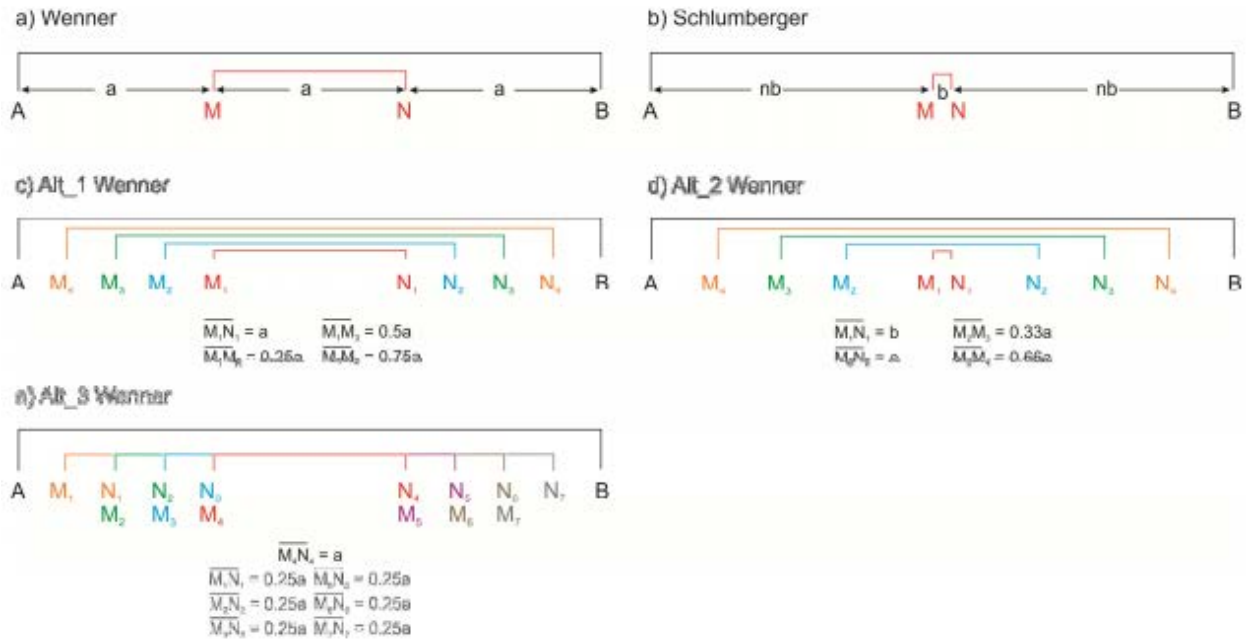


Figure 4.2. Adapted from Cubbage et al. 2017. This figure shows a stylized representation of the different arrays used in this project. The primary array type used in the HGI profiles was the Alt_3 Wenner array (e) in the above figure. This array collects a significantly larger amount of the data than the others, taking advantage of the plethora of electrodes between the transmitting pair that are typically unused in normal configuration. This technique increases resolution as well as provides a more robust final model. (Source: Cubbage et al. 2017).

4.4 Results:

4.4.1 Line H0.

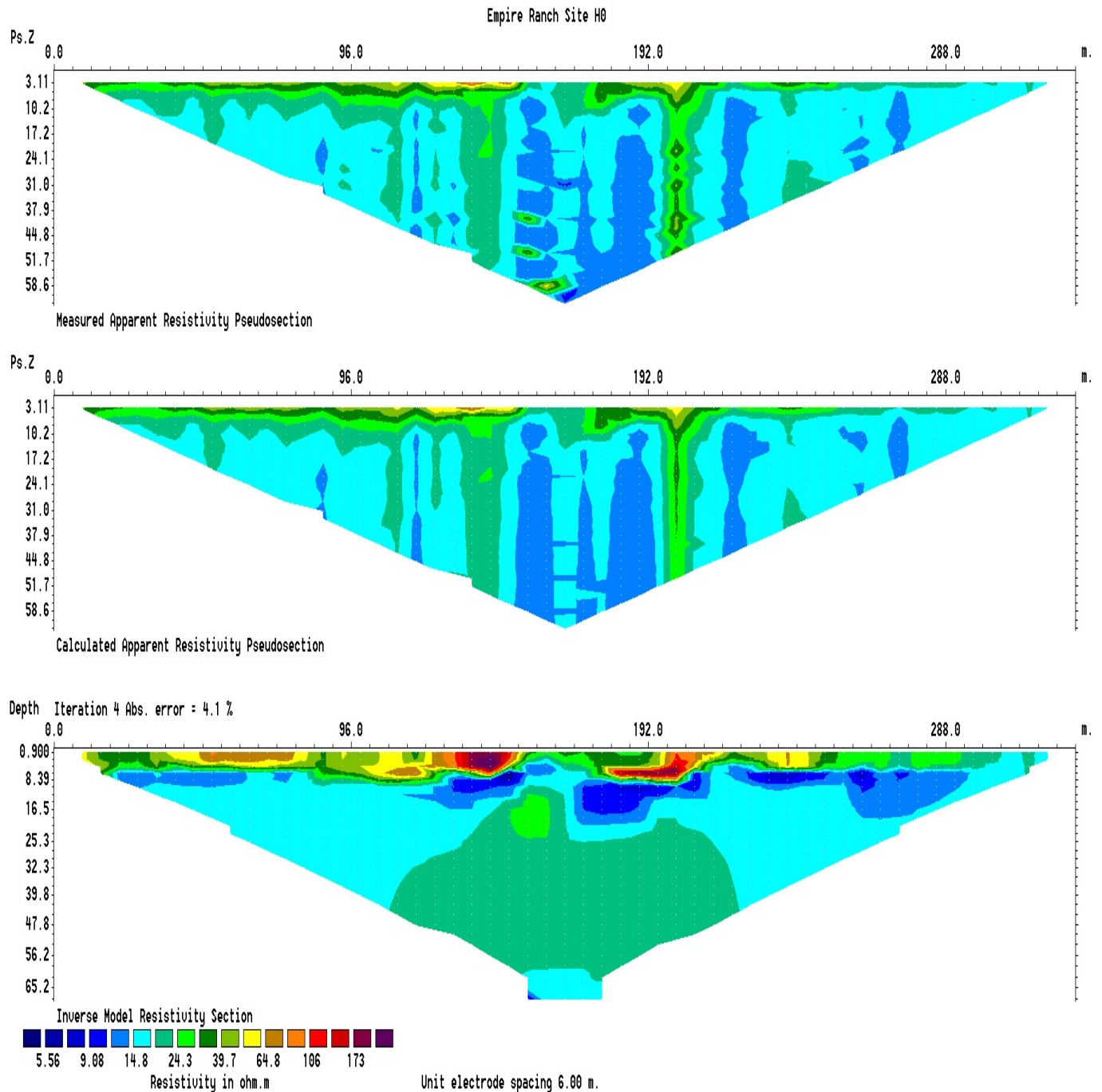


Figure 4.3. Line H0. The resistivity model for line H0 (Figure 4.3) shows a thin, high-resistivity layer immediately beneath the surface, underlain by a non-continuous layer of low resistivity. The low resistivity layer could represent water-saturated clays or soils.

4.4.2 Line H1.

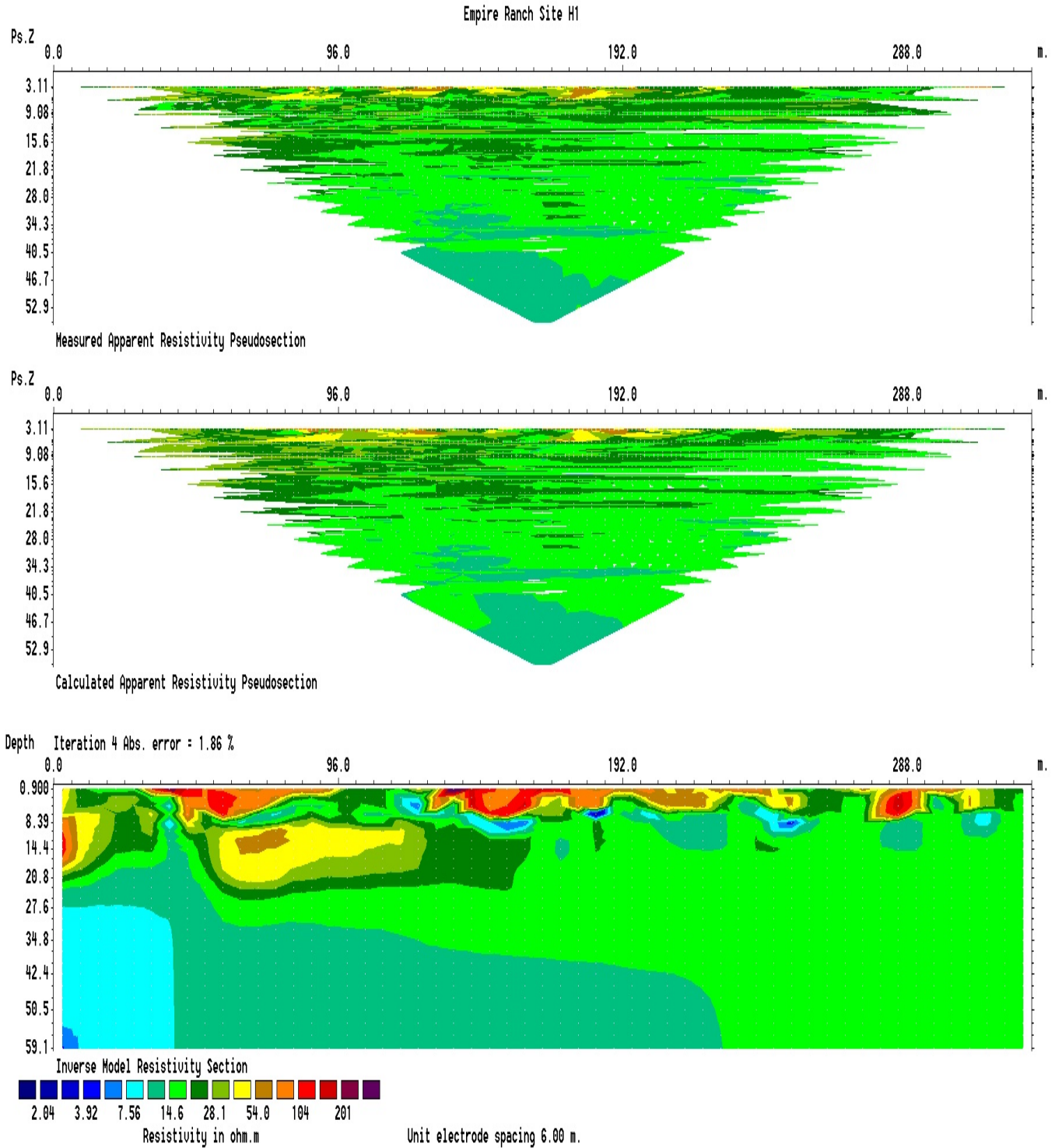


Figure 4.4. Line H1. The resistivity model for line H1 (Figure 4.4) shows a thin, high-resistivity layer immediately beneath the surface, underlain by a non-continuous layer of lower resistivity.

4.4.3 Line H2.

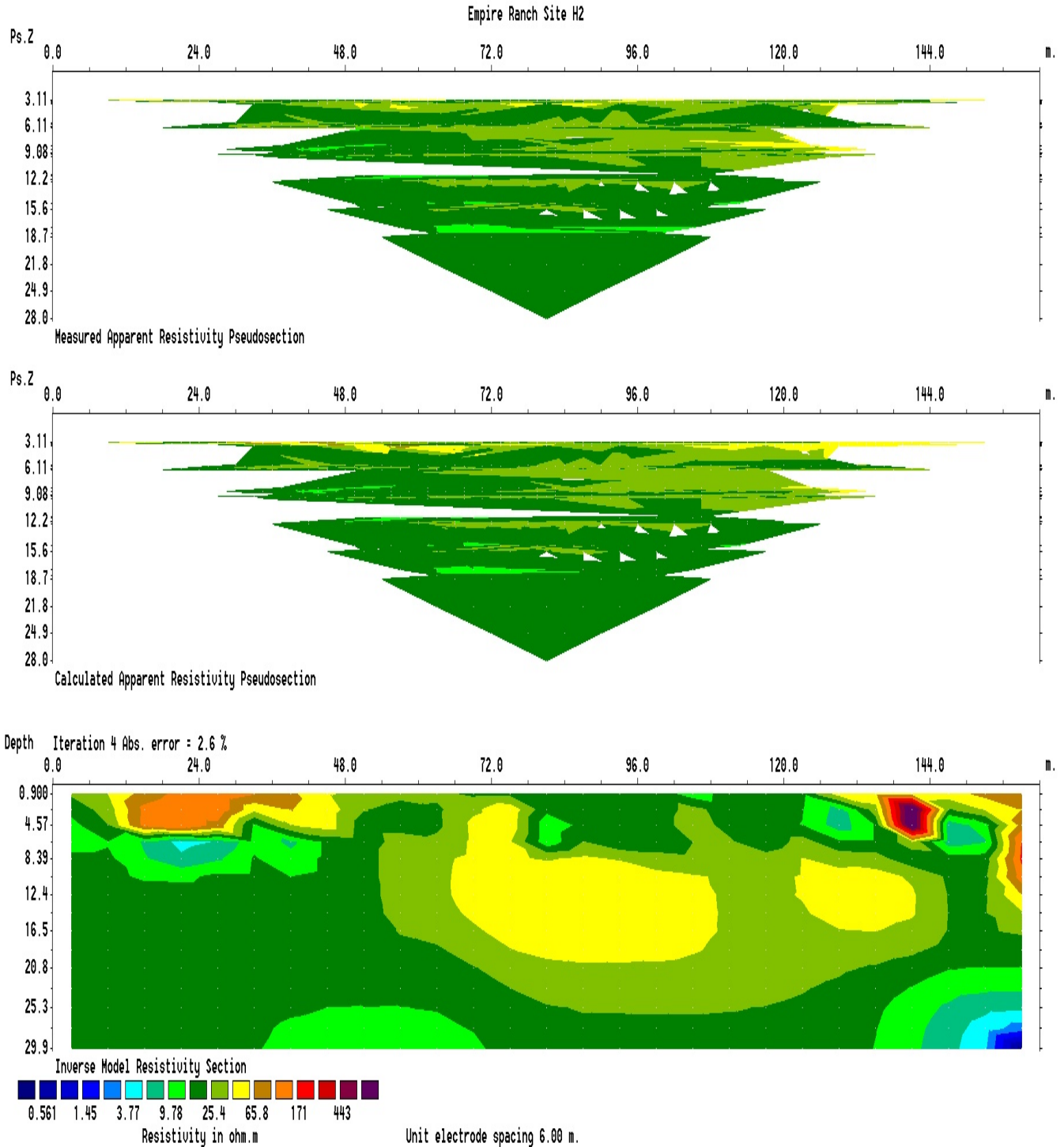


Figure 4.5. Line H2. The resistivity model for line H2 (Figure 4.5) shows a consistently high resistivity throughout the subsurface, with two pockets of particularly high resistivity at the surface. These pockets of higher resistivity may represent rock units of lower porosity.

4.4.4 Line H3.

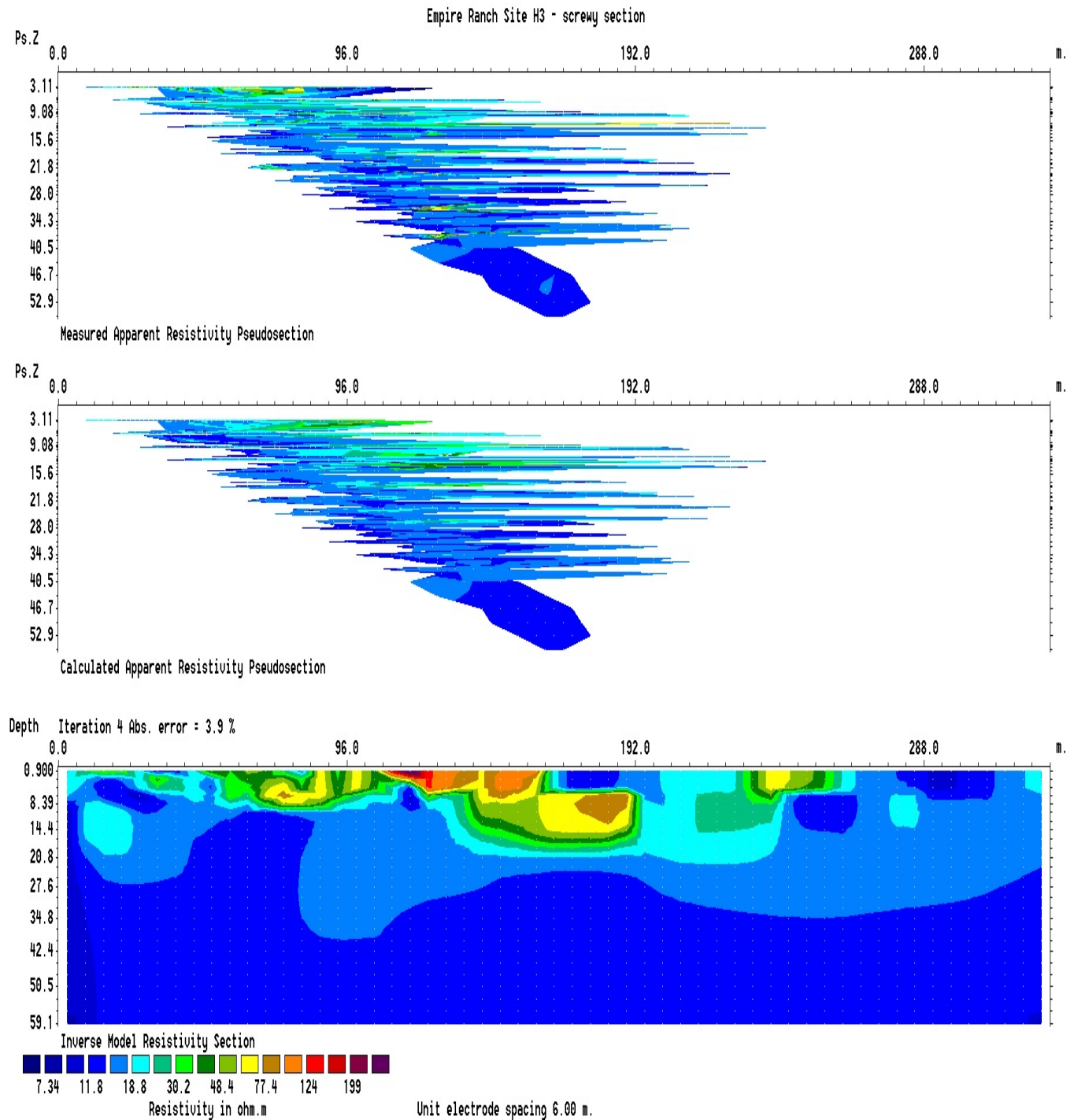


Figure 4.6. Line H3. The resistivity model for line H3 (Figure 4.6) shows a thin, non-continuous, high resistivity layer immediately beneath the surface, underlain by a layer of lower resistivity that occasionally breaks through the high resistivity layer. The low resistivity layer could represent water-saturated clays or soils.

4.4.5 Line H5.

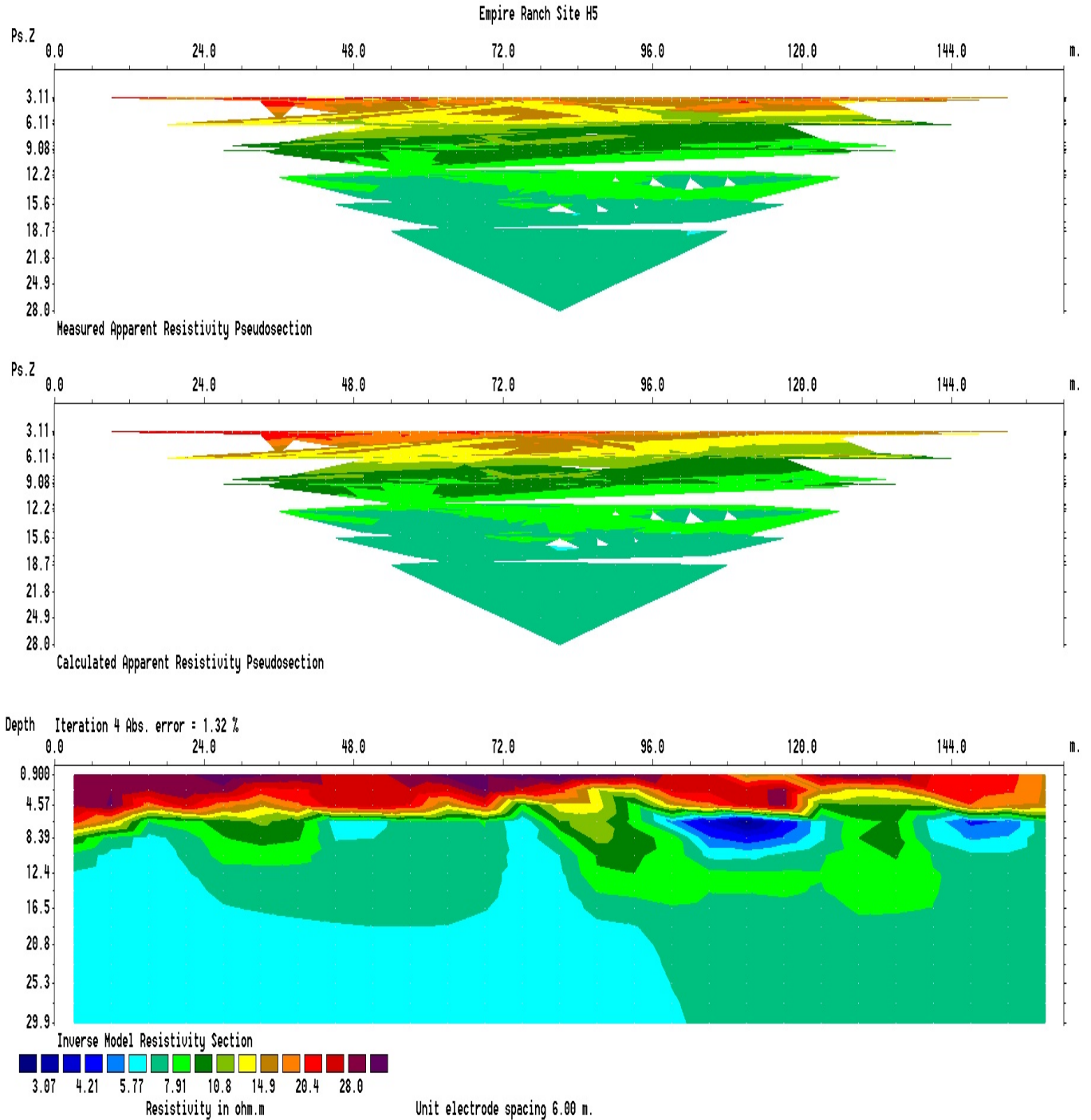


Figure 4.7. Line H5. The resistivity model for line H5 (Figure 4.7) shows a thin, high resistivity layer immediately beneath the surface, underlain by a layer of lower resistivity that occasionally breaks through the high resistivity layer. The low resistivity layer could represent water-saturated clays or soils.

4.4.6 Line H6.

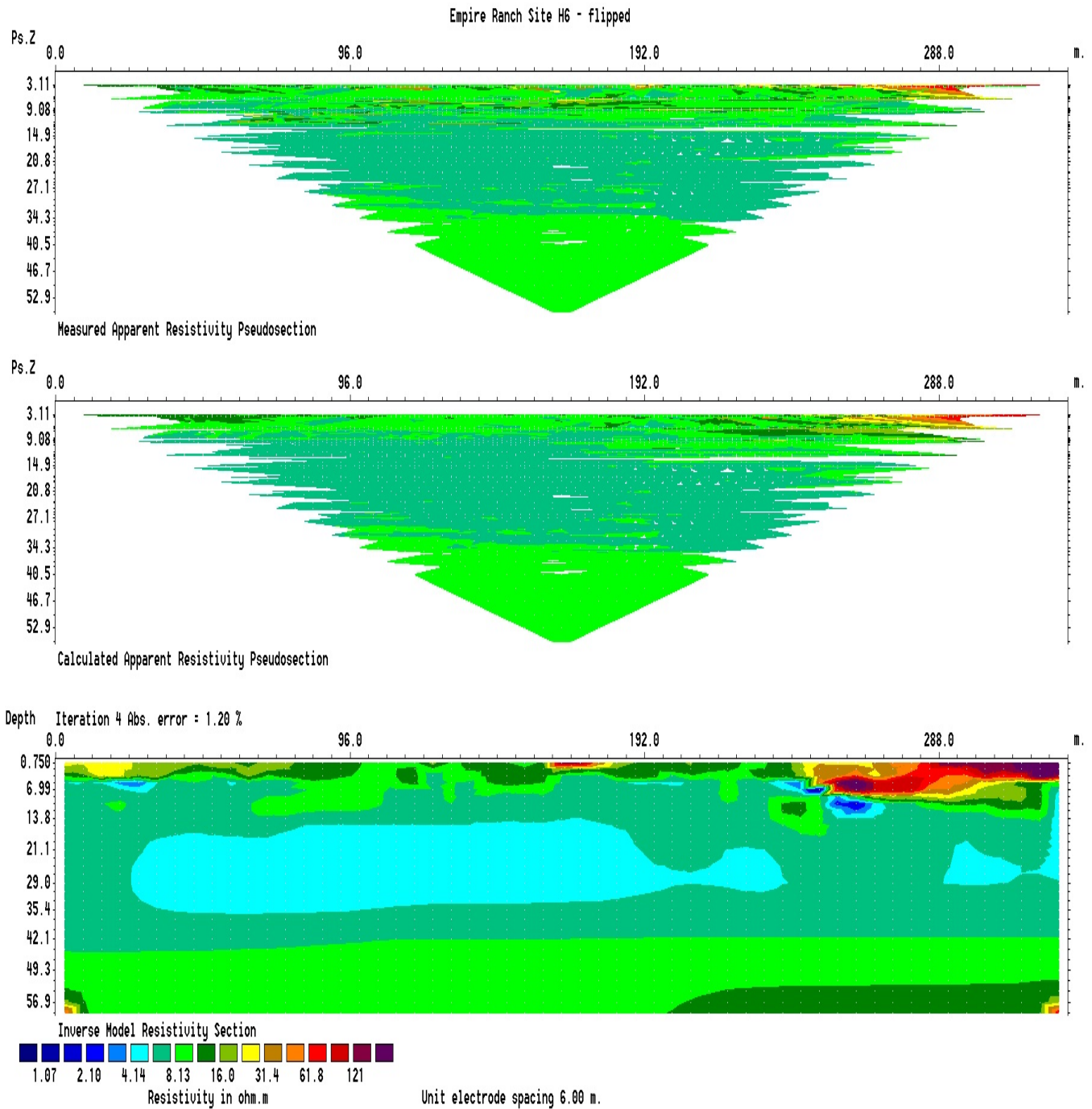


Figure 4.8. Line H6. The resistivity model for line H6 (Figure 4.8) shows a thin, relatively low resistivity layer immediately beneath the surface, underlain by a layer of lower resistivity that occasionally breaks through the high resistivity layer. The lower resistivity layer could represent water-saturated clays or soils, while the slightly higher resistivity layer could represent a dryer extension of the same layer.

4.4.7 Line H7.

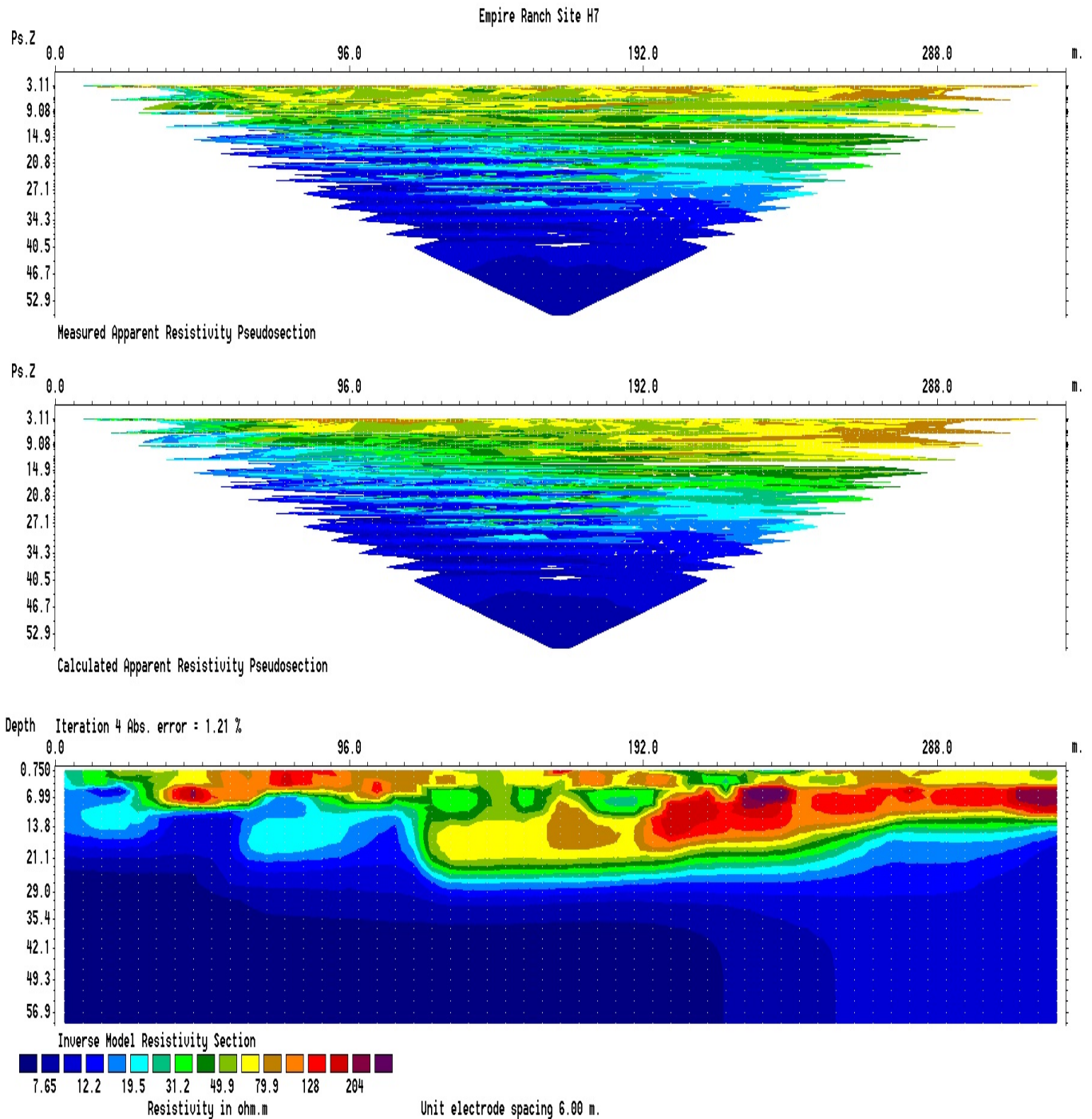


Figure 4.9. Line H7. The resistivity model for line H7 (Figure 4.9) shows a high resistivity layer immediately beneath the surface, underlain by a layer of significantly lower resistivity. The low resistivity layer could represent water-saturated clays or soils, while the high resistivity layer could represent the Vadose zone.

4.4.8 Line H8.

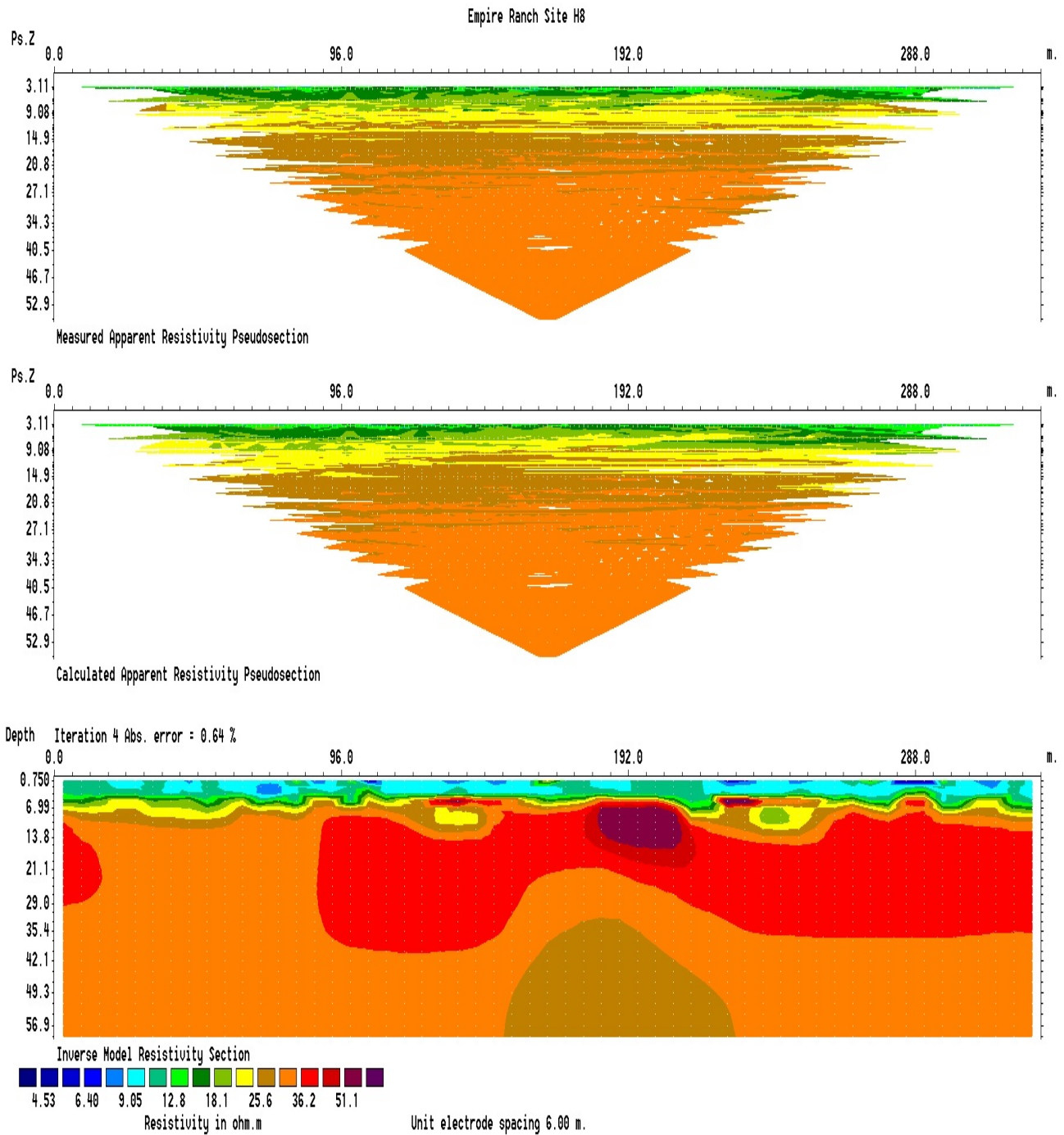


Figure 4.10. Line H8. The resistivity model for line H8 (Figure 4.10) shows a low resistivity layer immediately beneath the surface, underlain by a layer of higher resistivity. The low resistivity layer could represent water-saturated clays or soils characteristic of the cienegas, while the high resistivity layer could represent compacted clays or other low-porosity material.

5. Empire Ranch Headquarters (HQ) Interpretation

5.1 Introduction

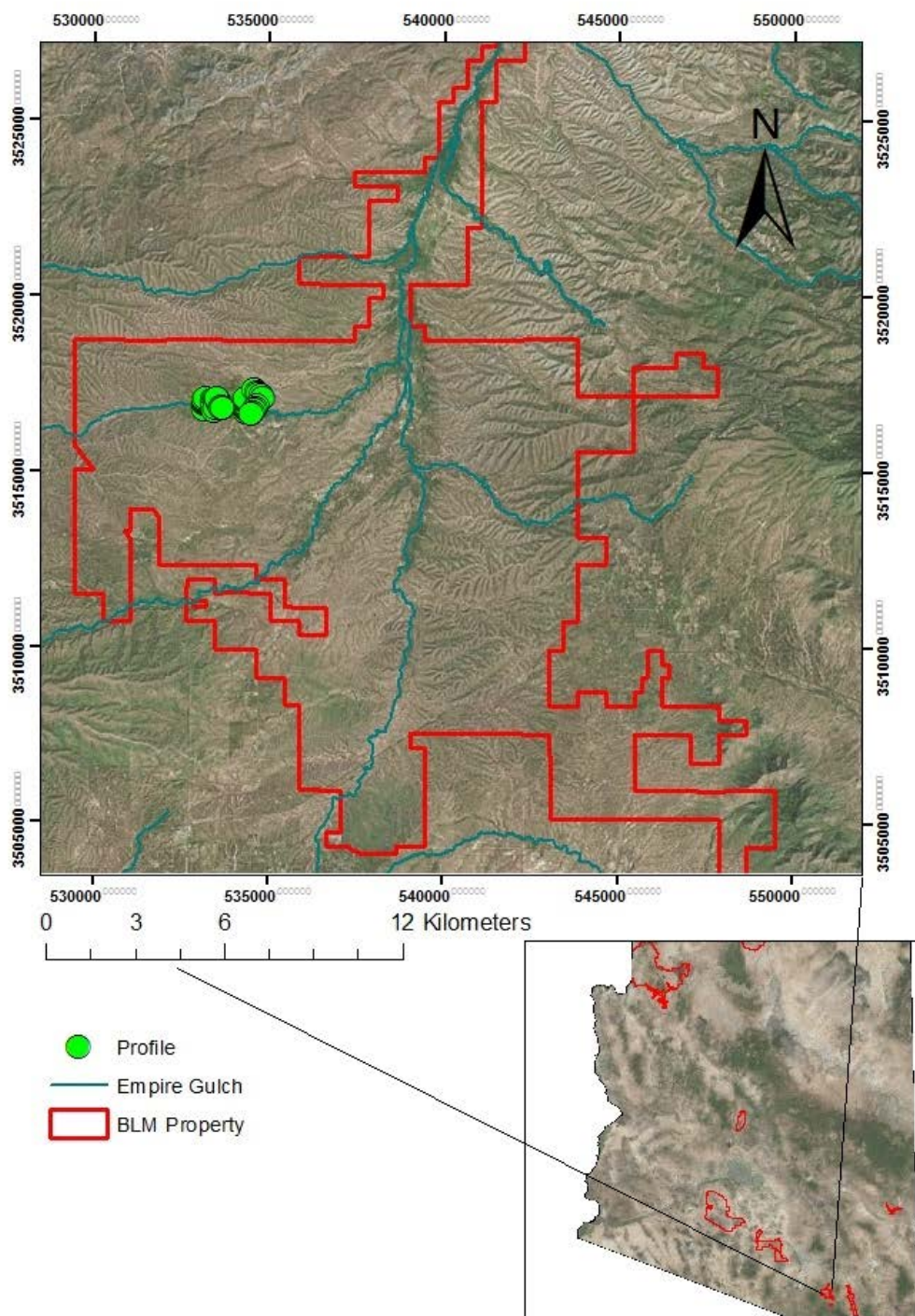
For interpretation purposes, the Direct current (DC) resistivity surveys can be divided into two distinct groups based on geographic location: the Empire Ranch Headquarters (HQ) and the Cieneguita Complex. Seven Hydrogeophysics Inc. (HGI) and two Zonge International profile lines were surveyed in the Empire Ranch HQ area; two of these lines were coterminous (H5 and Z2), allowing for a direct comparison between the two instrumentation setups used in the study. Due to the sequential nature of the profile lines, it was also possible to project the survey results onto a single resistivity cross section to aid in interpretation.

5.2 Location

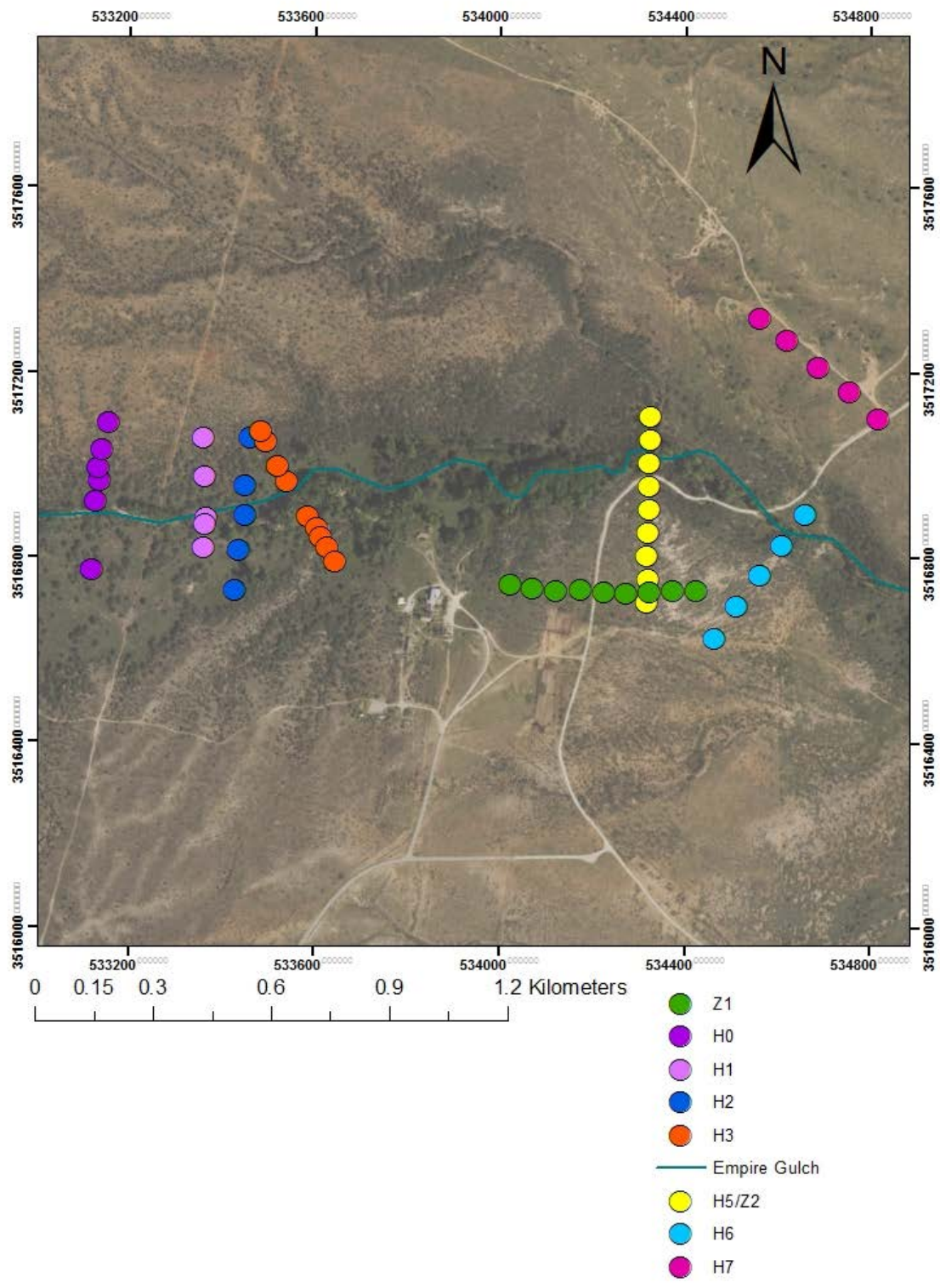
Survey data in the Empire Ranch HQ area were collected in close proximity to Empire Gulch, to the northwest and northeast of the Empire Ranch HQ. HGI profile lines were numbered H0 through H7, from west to east, with the exception of line H4, which was planned but not collected. Zonge profile lines were also numbered Z1 and Z2 from west to east. Lines H5 and Z2 were coterminous. Lines H0, H1, H2, and H5/Z2 followed general north-south trends, while line Z1 ran from west to east. Lines H3 and H7 ran from northwest to southeast, and H6 ran from southwest to northeast. Altogether, seven lines (H0, H1, H2, H3, H5/Z2, and H6) crossed Empire Gulch. See Table 5.1 for UTM coordinates of the profile lines, and Maps 5.1 through 5.4 for their locations.

Table 5.1

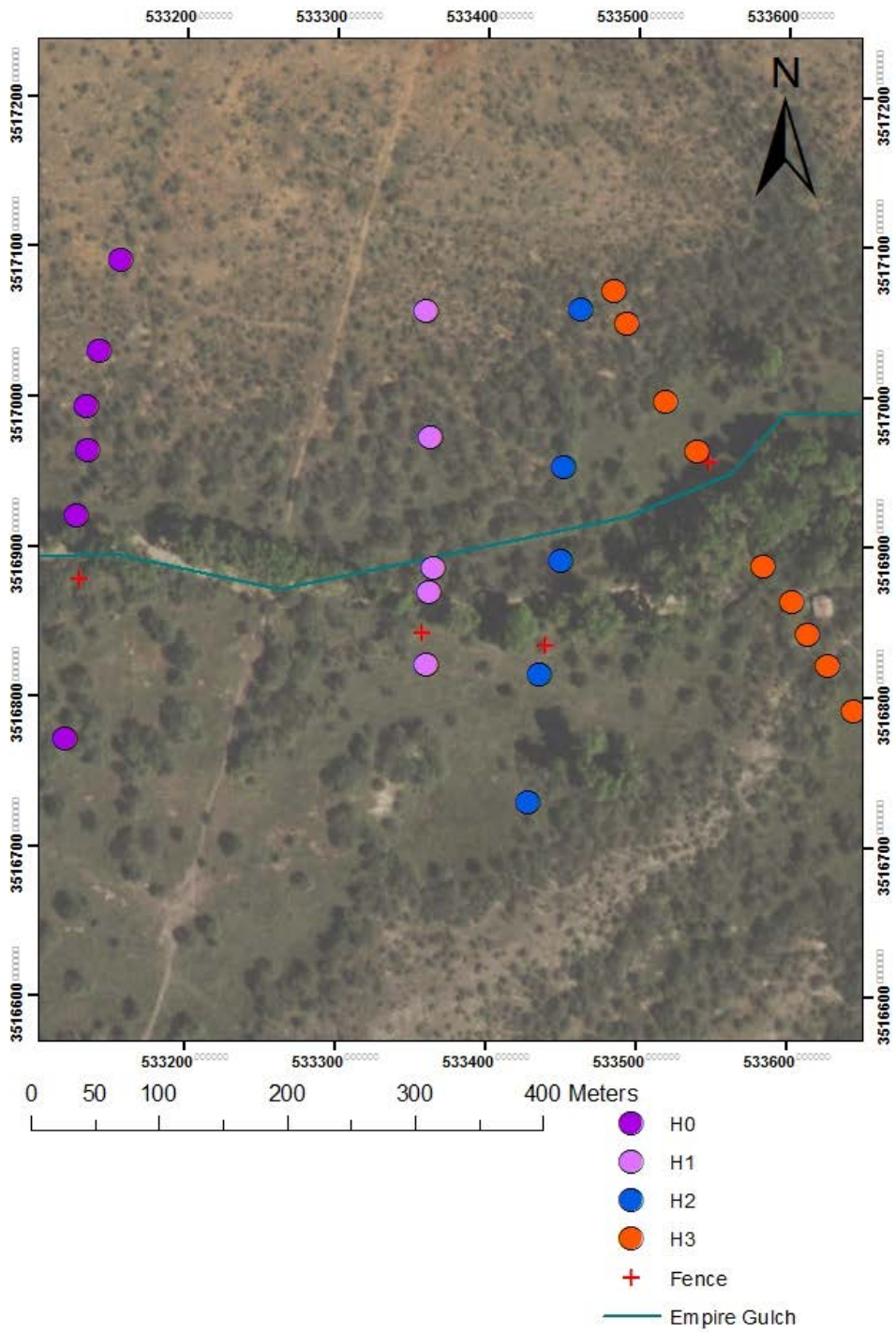
Profile Label	Line Start	Line End
H0	533120E, 3516772N	533156E, 3517091N
H1	533360E, 3516822N	533359E, 3517058N
H2	533428E, 3516730N	533462E, 3517059N
H3	533644E, 3516791N	533484E, 3517072N
H5/Z2	534333E, 3516699N	534324E, 3517107N
H6	534660E, 3516894N	534463E, 3516627N
H7	534814E, 3517103N	534558E, 3517320N
Z1	534429E, 3516738N	534023E 3516741N



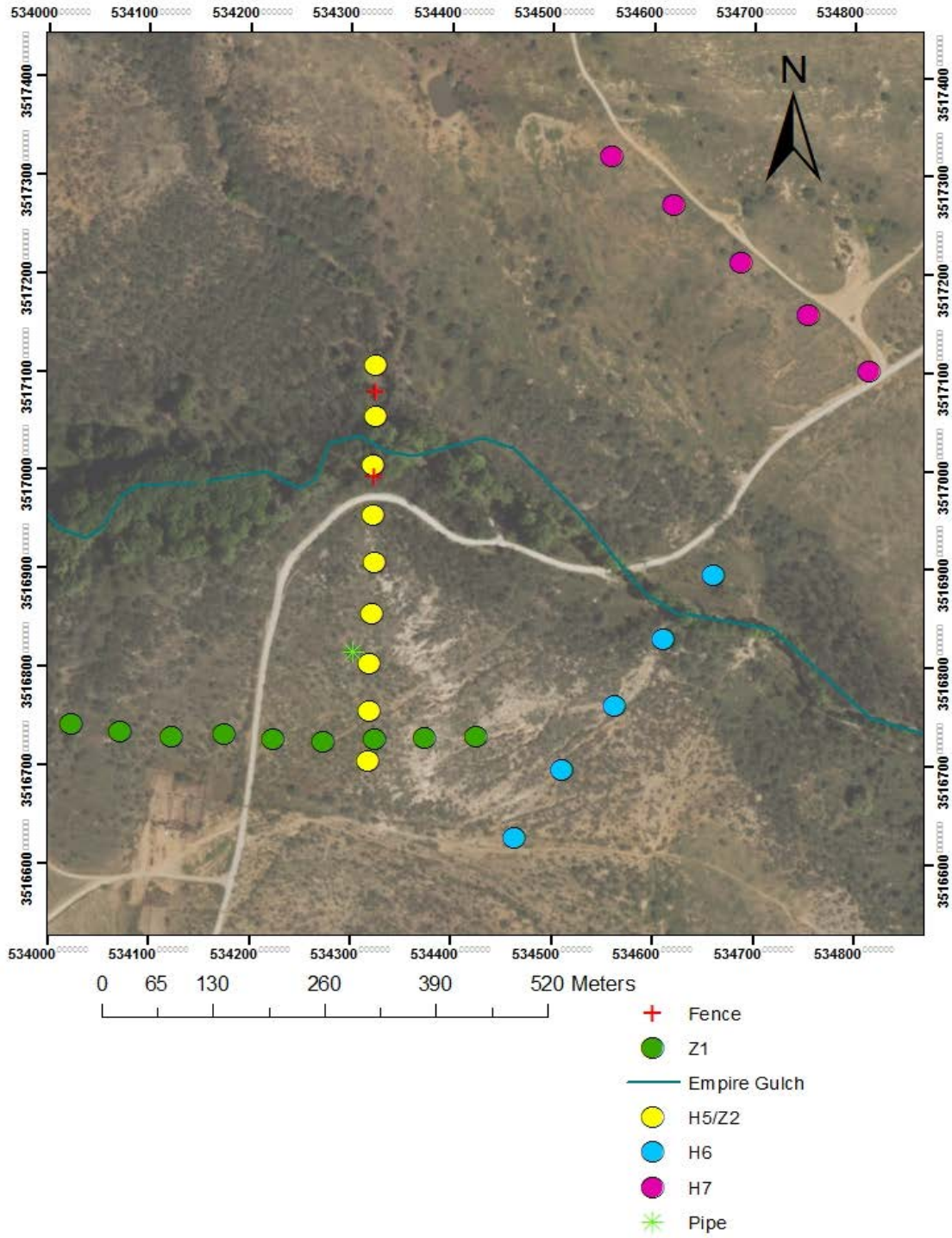
Map 5.1 Empire HQ Location.



Map 5.2 Locations of profile lines near the Empire Ranch HQ.



Map 5.3 Profile lines H0-H3.



Map 5.4 Profile lines Z1, H5/Z2, H6, and H7.

5.3 Side-by-Side Comparison

The surveys conducted at profile lines H5 and Z2 were coterminous, allowing for a side-by-side comparison of the resistivity data collected using the HGI and Zonge instrumentation. Since the Zonge data were collected using an array with a larger a-spacing, the depth of investigation is considerably larger than the HGI data. Additionally, a technical issue with the HGI equipment during data collection corrupted half of the H5 survey data, resulting in a model approximately half of the length of the Zonge data.

Nevertheless, the general subsurface trends in the inverted survey data compare well, each displaying a surface layer of resistive material underlain by a lower resistivity layer beneath. The models are not identical, however; some of this may be attributed to slight offsets between the locations of the survey lines collected with each set of equipment.

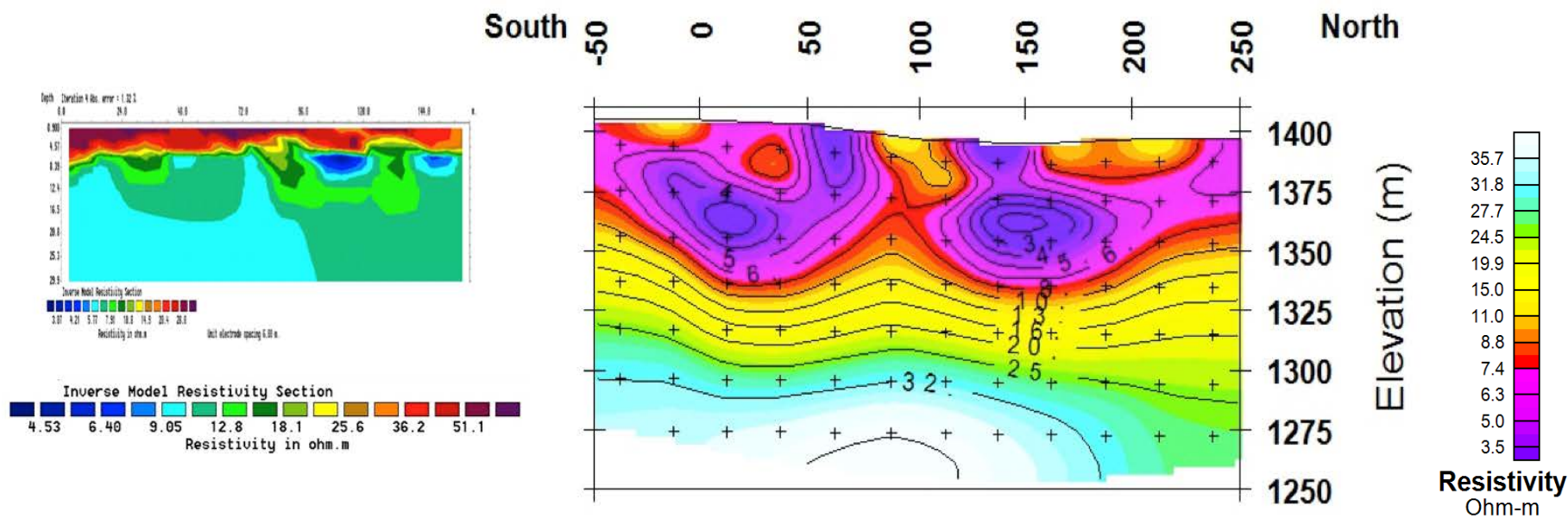


Figure 5.1 Side-by-side comparison of resistivity inversion models for lines H5 (left) and Z2 (right).

5.4 Projected Resistivity Cross Sections

Because most surveys in the Empire Ranch HQ area followed similar trends and were collected in or near Empire Gulch, the survey results could be projected onto a single east-west trending line to create a hypothetical resistivity cross section of the subsurface along Empire Gulch. Inversion models for the individual lines were incorporated into the projected line in two ways, producing two cross sections. The first cross-section, seen in Figure 5.2, was produced by cropping the left and right sides of the inversion models, while the second, seen in Figure 5.3, was produced by compressing the inversion models along the horizontal axis. The Zonge data, which were produced using a different color scale, were not included in the projected cross sections, so as not to give the reader distracting visual impressions about the regional resistivity trends.

As demonstrated by the cross sections, lines H0 through H3 exhibit similar general resistivity trends, with a thin resistive layer of 60 to 80 Ω -m extending between five and ten meters into the subsurface, underlain by a more conductive layer ranging from 20 to 25 Ω -m. Moving east along the projected line, however, there is a radical departure from this pattern: Lines H5/Z2 and H6 exhibit a thin layer of 15 to 20 Ω -m extending five meters below the surface, underlain by a highly conductive layer of 5 Ω -m. Further east, Line H7 displays yet another change, with a thick resistive layer of 80 Ω -m extending 25 meters into the subsurface, underlain by the same highly conductive 5 Ω -m layer. The extremely conductive lower layer evident in the eastern reaches of the projected line is unusual for the alluvial basins of Southern Arizona, and could indicate the presence of significant clay deposits.

We note that the IP phase angles in the Zonge data are very low in the Empire Ranch HQ area. The interpretation of these data is simply that there is no indication of polarizable material, such as clay-rich earth.

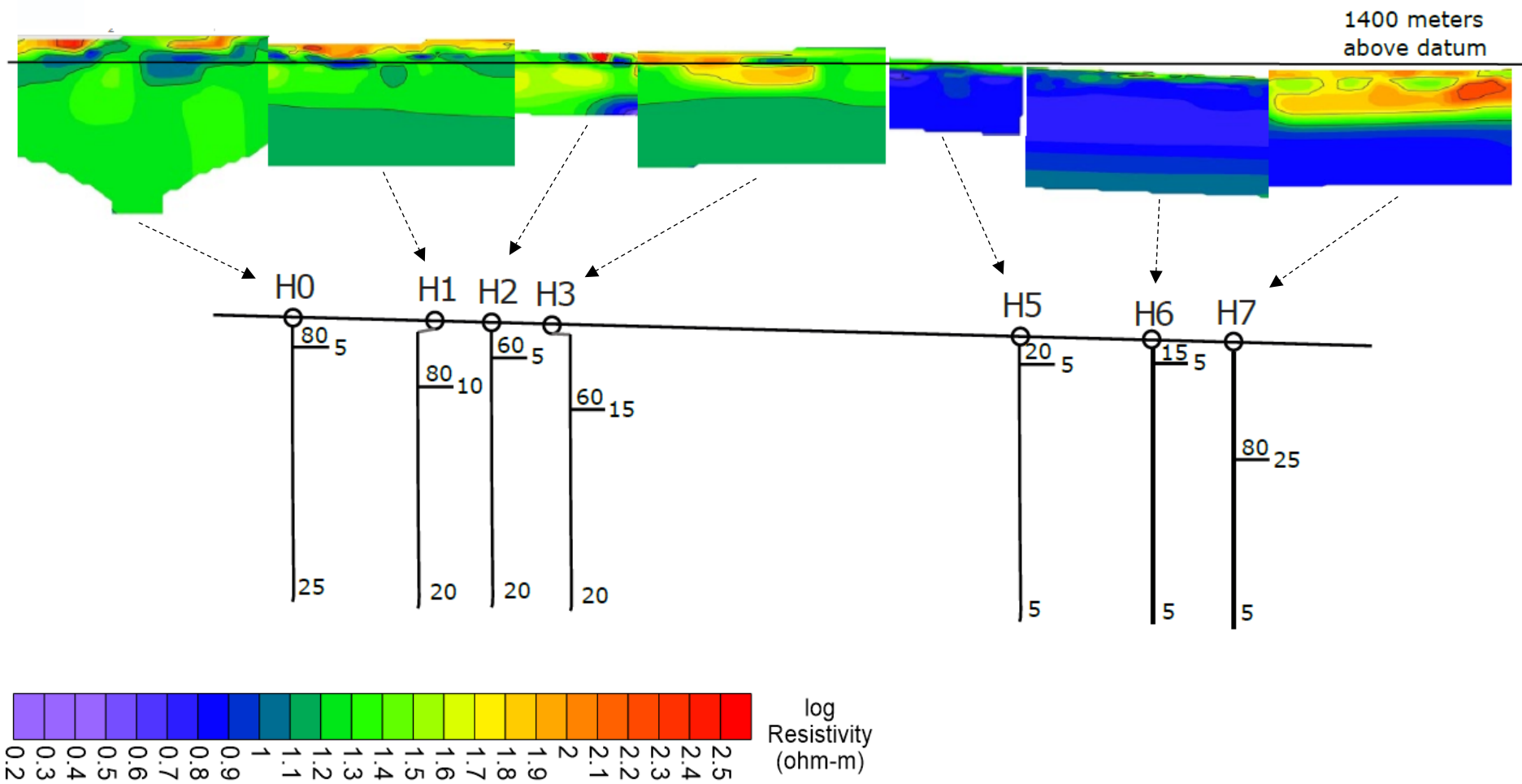


Figure 5.2 Projected resistivity cross section produced with cropped inversion models. Values next to the vertical lines in the bottom figure are the layer resistivities in Ohm-m. Values next to the short horizontal lines in the bottom figure are the layer depths in meters.

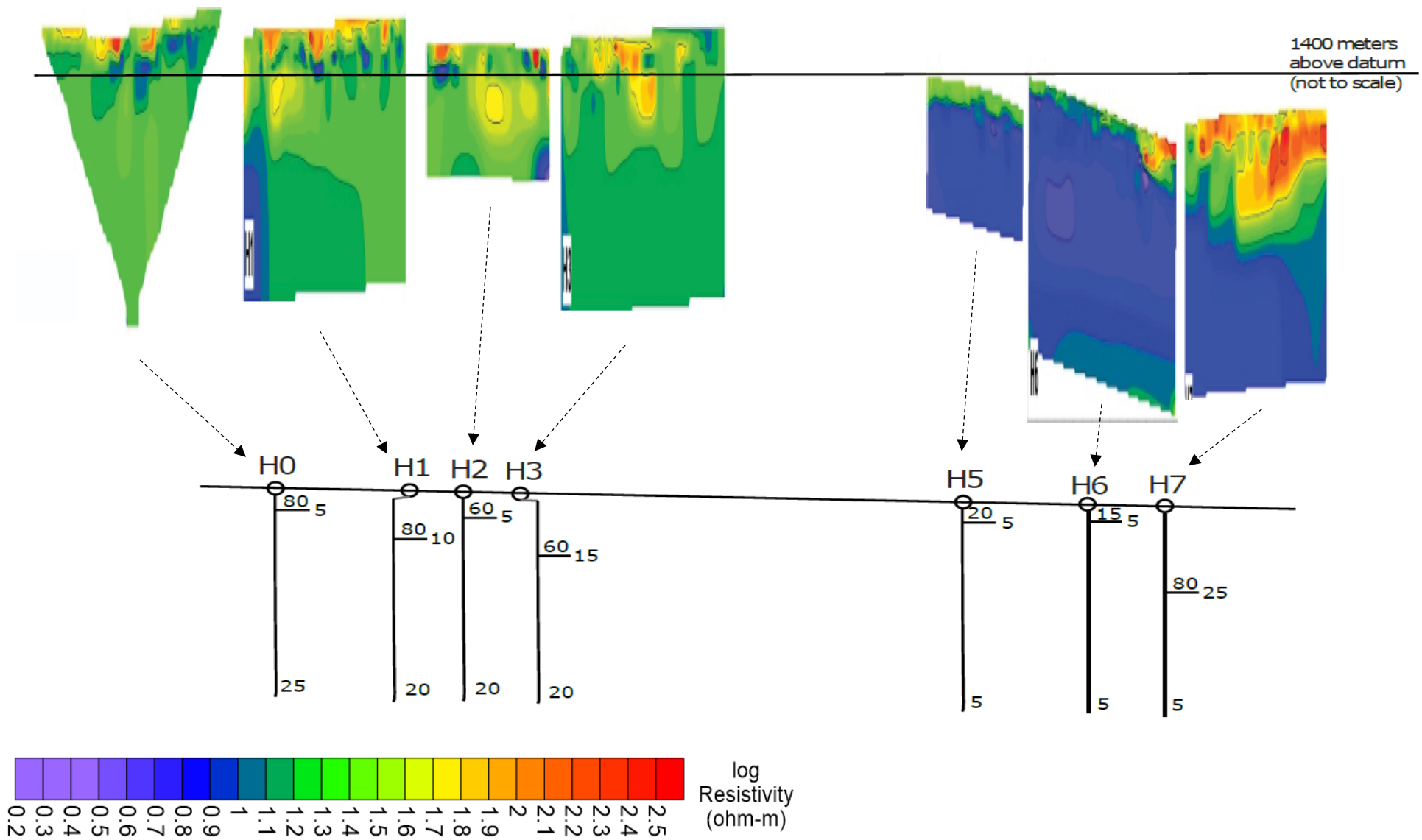


Figure 5.3 Projected resistivity cross section produced with compressed inversion models. Values next to the vertical lines in the bottom figure are the layer resistivities in Ohm-m. Values next to the short horizontal lines in the bottom figure are the layer depths in meters.

6. Cieneguita Cienega Complex Interpretation

6.1 Introduction

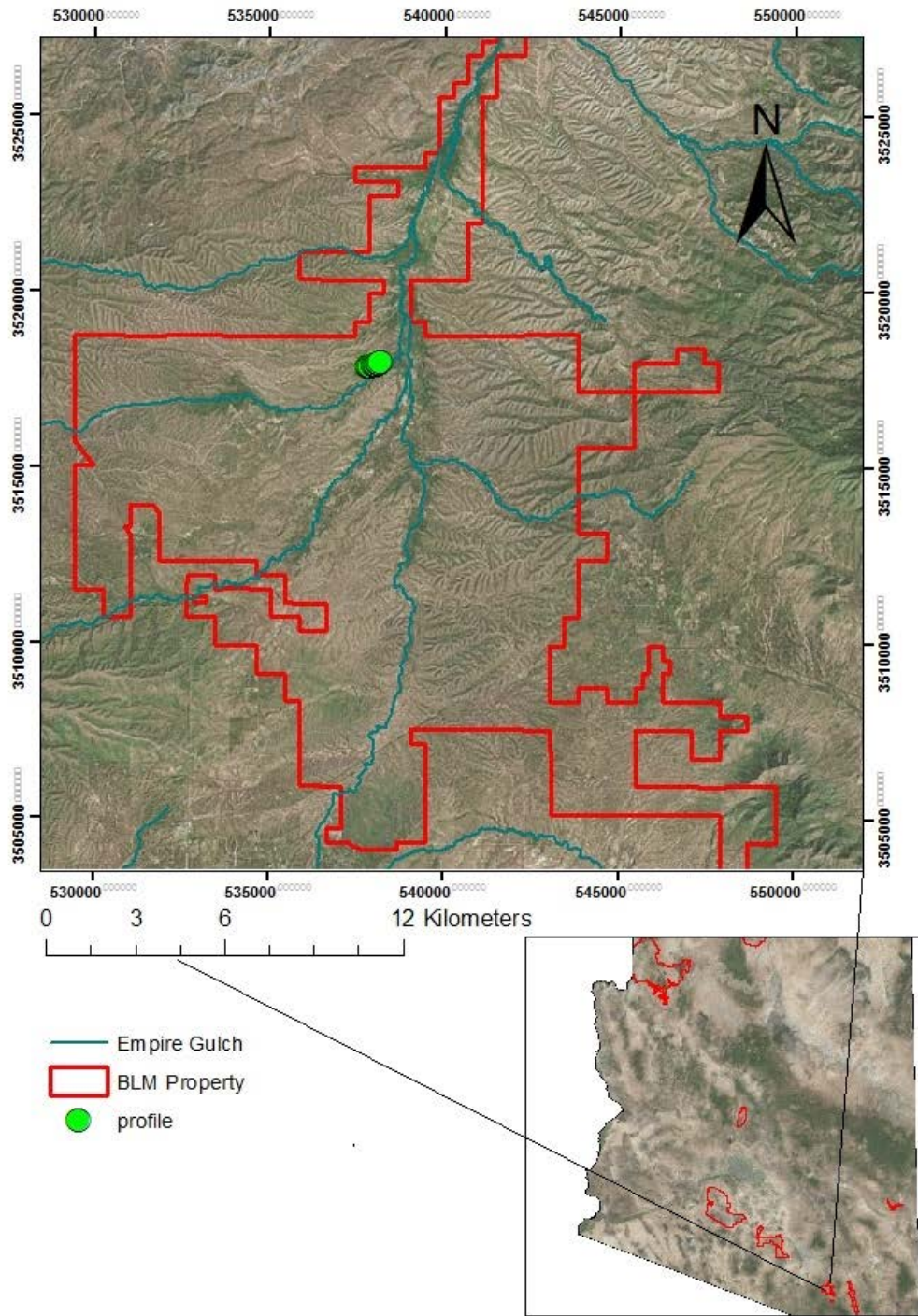
For interpretation purposes, the Direct current (DC) resistivity surveys can be divided into two distinct groups, based on geographic location: the Empire Ranch Headquarters (HQ) and the Cieneguita Cienega Complex. Two coterminous profile lines were surveyed in the Cieneguita area, one using Zonge International equipment (Z3) and one using Hydrogeophysics Inc. (HGI) equipment (H8), allowing for a direct comparison between the two instrumentation setups. Additional subsurface data for the area were available from logs of a nearby well, named D-19-17 10BCA. The logs used were resistivity, gamma ray, neutron, and 3D velocity logs recorded on March 18, 1975. The information from these well logs was used in conjunction with the resistivity data collected for this study to aid in interpretation.

6.2 Location

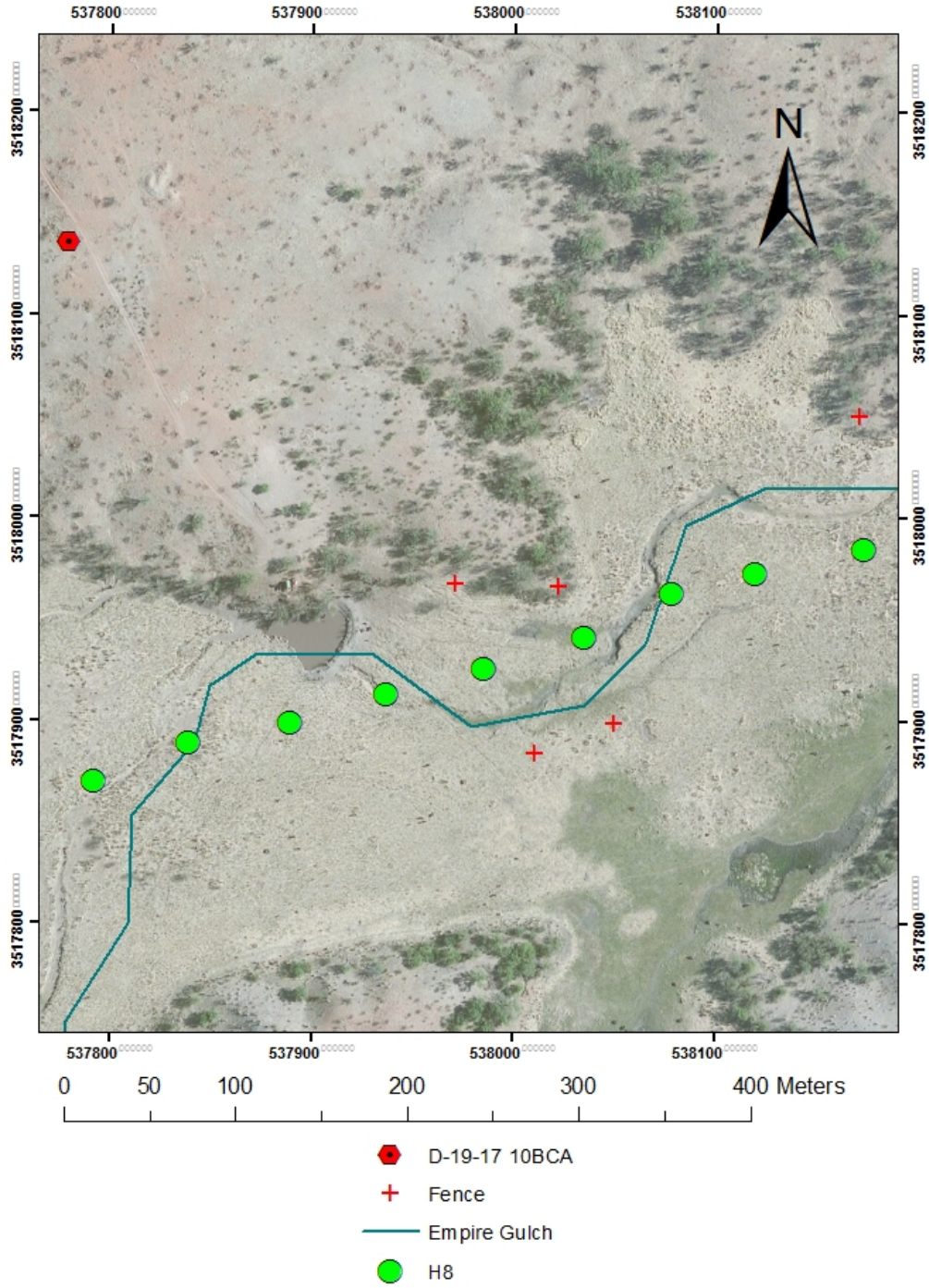
Survey data in the Cieneguita Complex were collected in Empire Gulch, northeast of the Empire Ranch HQ and west of Cienega Creek (Map 6.1). Line H8/Z3 runs in a general southwest-northeast trend between two fences. The well, D-19-17 10BCA, is located 180 meters northwest of line H8/Z3. See Table 6.1 below for the exact UTM coordinates of the profile lines and well, and Map 6.2 for their locations.

Table 6.1

Profile/Well Label	Line Beginning	Line End
Z3	537791E, 3517889N	538173E, 3517985N
H8	537791E, 3517889N	538173E, 3517985N
D-19-17 10BCA	537779E, 3518135N	N/A



Map 6.1 Cieneguita Complex Location.



Map 6.2 Locations of H8, Z3, and D-19-17 10BCA.

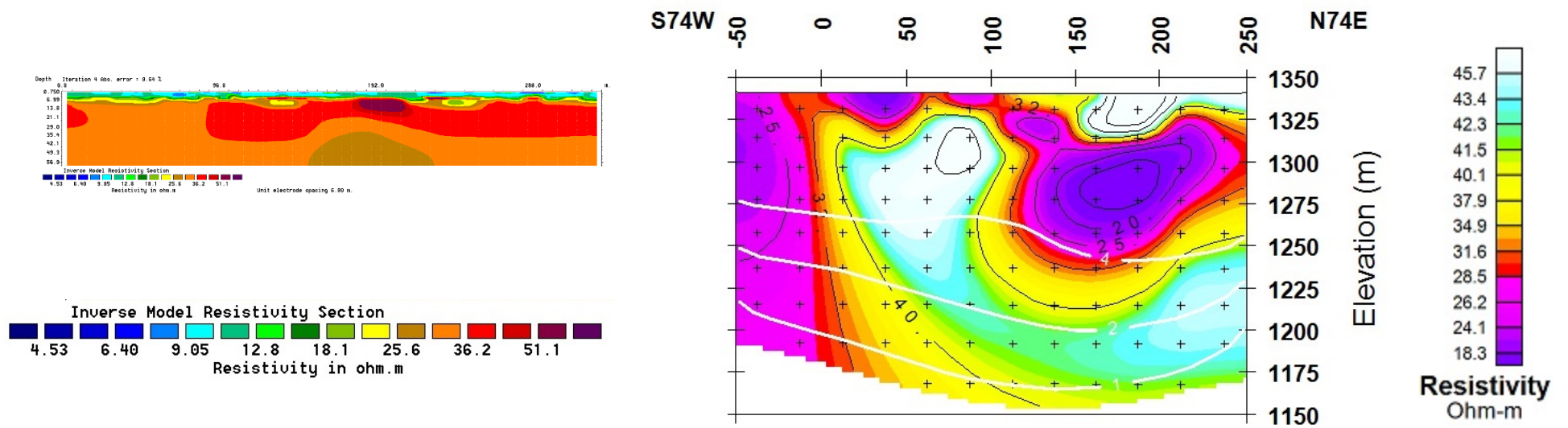


Figure 6.1. Side-by-side comparison of resistivity inversion models for lines H8 (left) and Z3 (right).

6.3 Side-By-Side Comparison

The surveys conducted at profile lines H8 and Z3 were coterminous, allowing for a side-by-side comparison of the resistivity data collected using the HGI and Zonge instrumentation (Figure 6.1). Since the Zonge data were collected using an array with a larger a-spacing, the depth of investigation is considerably larger than that of the HGI data.

Because of the different depth of investigation in the two surveys, the resolution of the near-surface layers is different. For example, the thin conductive layer present in the HGI model does not appear in the Zonge model, because of the larger a-spacing that was used. In general, the modeled resistivities over the entire cross section are similar (approximately 20 to 50 Ohm-m). This is typical for alluvium resistivities in the southwest US. The large-scale trends in resistivity are similar on the two sections. There are some differences near the edges of the sections, but the edges have limited resolution in the modeling, because there is limited measured data near the ends of these surveys.

We have not included the IP data in this interpretation chapter. The IP response at this location shows a large response throughout the modeled section. More modeling is required before this response can be interpreted. It is likely that this apparent high IP response may actually be caused by electromagnetic coupling.

6.4 Well Logs

Well logs are detailed records of geophysical, geological, and other properties collected directly from the formations penetrated by a borehole. To aid in interpretation, resistivity, gamma ray, neutron, and 3D velocity well logs from D-19-17 10BCA were gathered and analyzed.

Much like the surface resistivity surveys conducted for this study, resistivity is often logged in wells in order to assess the presence and properties of water and other pore fluids. Standard resistivity logs use 16- and 64-inch depths of investigation. The 16-inch resistivity measurement does not penetrate very far into the borehole wall, and is therefore affected by the mud used to drill the well, while the 64" measurement extends deep enough to measure the earth materials surrounding the well.

The D-19-17 10BCA resistivity log was recorded from 100 to 1242 feet in the well with both 16- and 64-inch depths of investigation (Figure 6.2). Resistivity logs are quite sensitive to changes in lithology and fluid content, but the recorded values for the well hover around 50 Ω -m for the interval 100-200 foot interval of interest in this study. This indicates that there is little variation in rock type at the depth intervals concerned in this study.

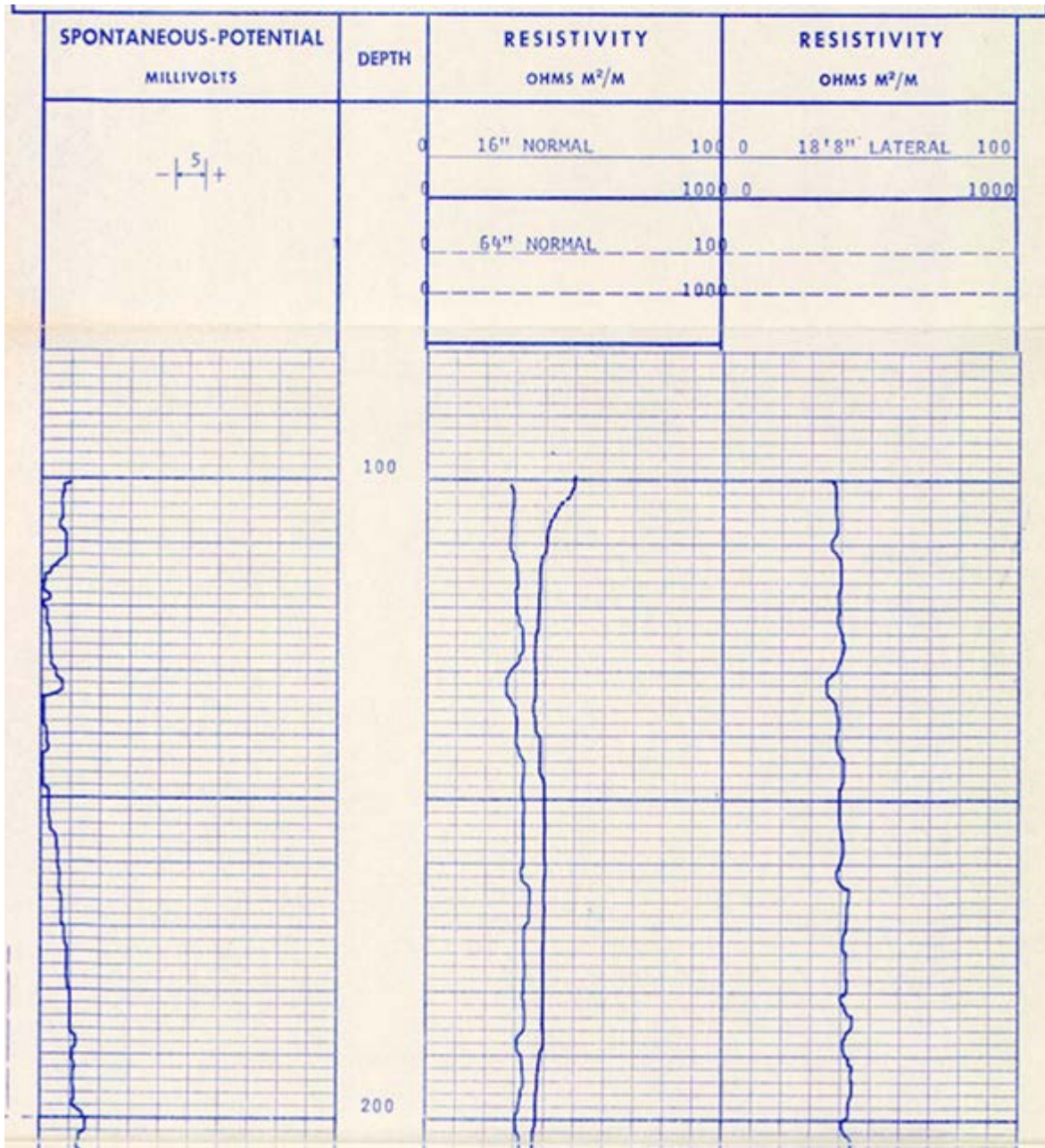


Figure 6.2 Well D-19-17 10BCA Resistivity Log.

Gamma ray logs record the natural radioactivity of the penetrated formation in API units. The depth of investigation is usually only a few inches, so the log normally measures the flushed zone. Because shales and clays are responsible for most natural radioactivity, gamma radiation is often a strong indicator of their presence. Nevertheless, there are other radioactive materials, such as carbonates and feldspar-rich rocks.

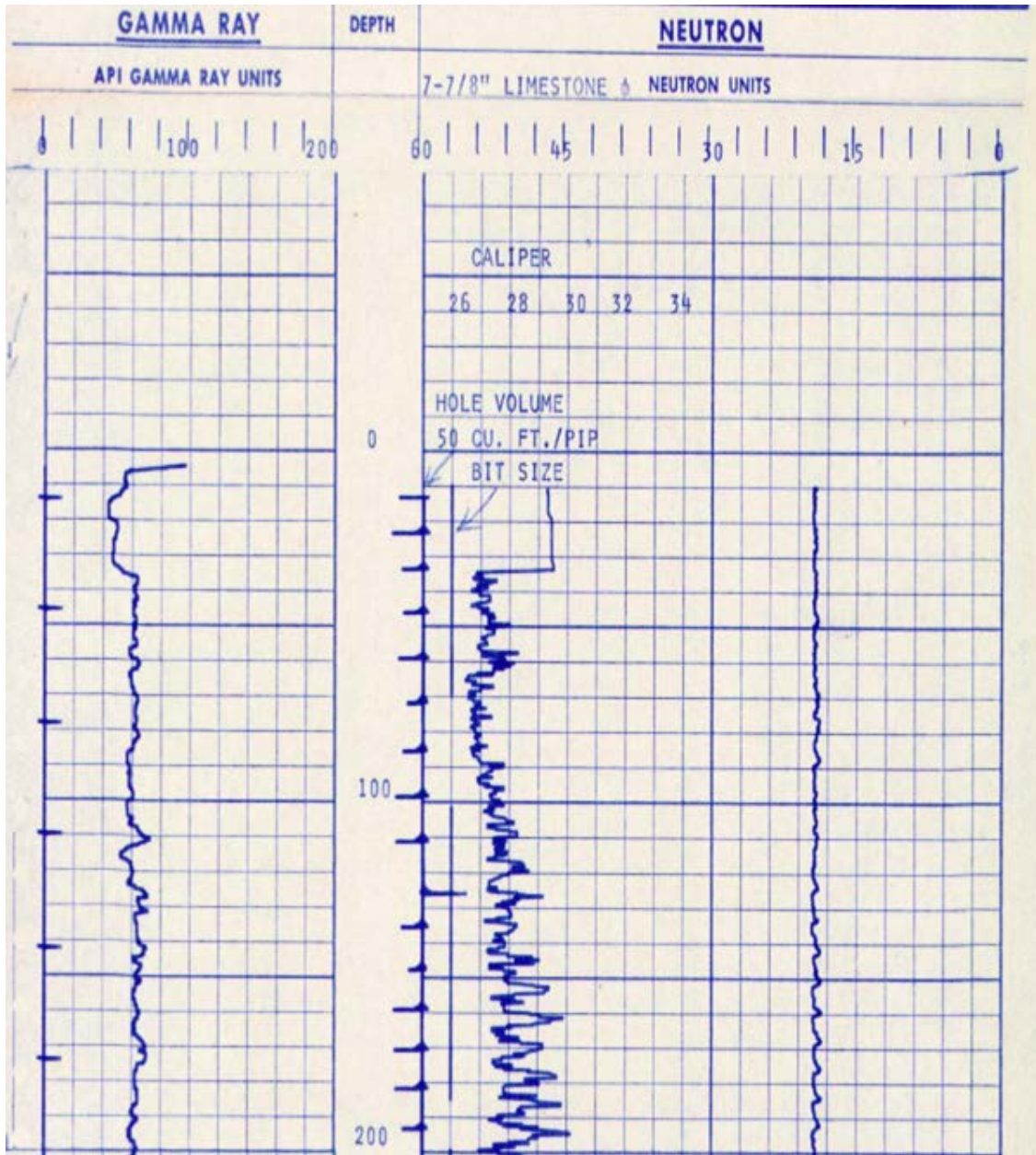


Figure 6.3 Well D-19-17 10BCA Gamma Ray and Neutron Log.

The gamma ray log for well D-19-17 10BCA is recorded from 10 to 1233 feet, but the measurement is clearly affected by the borehole casing for the first 30 feet (Figure 6.3). Much like the resistivity log, there is little deviation from the 60-API average in the first 200 feet.

Neutron logs measure the porosity of a formation through the detection of hydrogen atoms. This is accomplished by bombarding the rock with high-energy neutrons, causing neutron scattering and the emission of gamma rays, which are in turn recorded as a count rate. Since neutrons are

absorbed more quickly in hydrogen, large amounts of hydrogen will diminish the count rate; because hydrogen is also more common in porous rocks, a low count rate indicates a high porosity. Surficial alluvium often has high porosities, but alluvium tends to decrease in porosity with increasing depth.

The neutron log for D-19-17 10BCA is recorded from 10 to 1233 feet, but the measurement is clearly affected by the borehole casing for the first 30 feet (Figure 6.3). Like the gamma ray log, the neutron log shows the low variability in the first 200 feet, almost the entire the log has values of 20 neutron porosity units.

The 3-D velocity logging system utilizes transmitting and receiving transducers placed at a known displacement from one another. The transmitter generates pulses of a specified bandwidth at a constant rate; the receiving transducer detects these pressure waves and converts them into electric signals, which are relayed to recording equipment at the surface. The total wave train, including pressure, shear, and boundary waves, can be displayed as a variable density by a specially designed camera. The velocity log for D-19-17 10BCA showed little variation in velocity, indicating a homogenous lithology in the first 200 feet (Figure 6.4).

Altogether, the well logs implied that the subsurface at the well site was homogeneous, consolidated, moderately resistive, and not strongly radioactive. The information from the well logs, together with the resistivity inversion models, suggest that the subsurface geology of the Cieneguita Complex can be interpreted as Late Tertiary and Quaternary basin fill deposits (Figure 6.5).

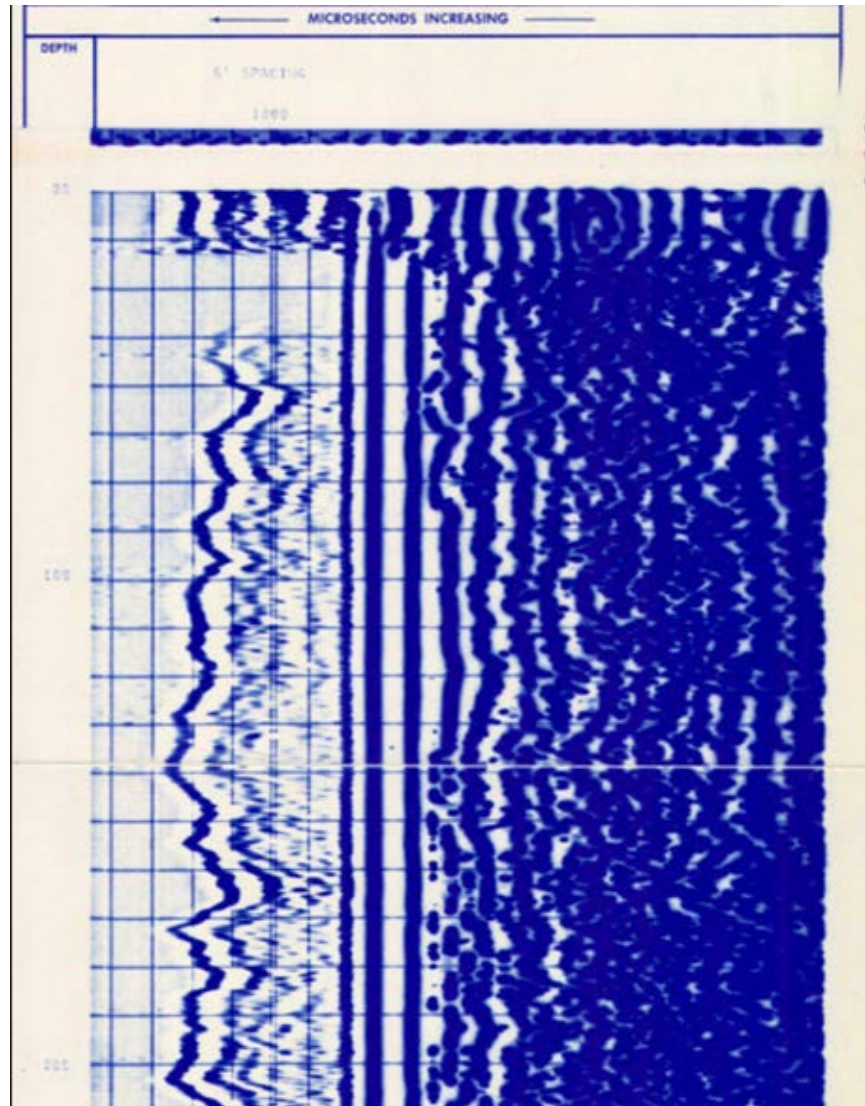


Figure 6.4 Well D-19-17 10BCA Velocity log.

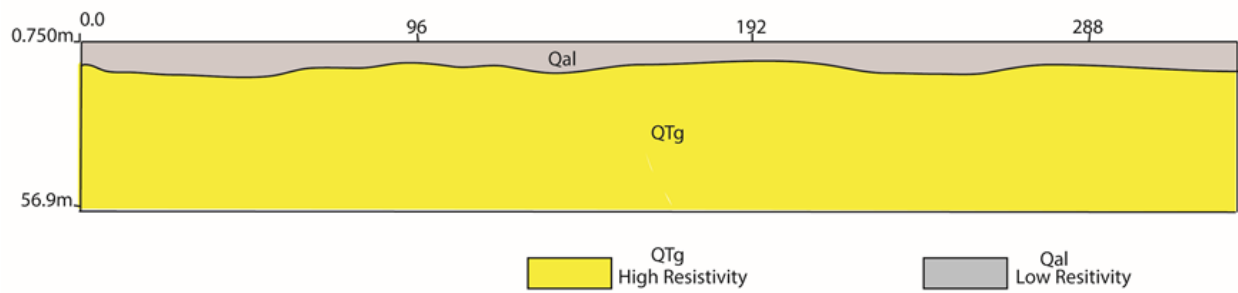


Figure 6.5 Proposed lithology of the Cieneguita Complex study area.

7. Conclusions

Although the Zonge International Inc. and the HGI Inc. resistivity surveys were conducted separately with two different methods, the results from each survey were compared and found to have similar conclusions. Starting from the west of the Empire Ranch Headquarters, H0 and H1 has a thin layer, about 5 to 10 meters in depth with a resistivity of 80 Ohm-m overlaying a 20 to 25 Ω -m resistivity layer. H2 and H3 have an increasing layer of 5 to 15 meters in depth with a resistivity of 60 Ohm-m overlaying a 20 Ohm-m resistivity layer. Moving to the east, H5/Z3 and H6 appear to have a surface resistivity of 15 to 20 Ohm-m overlaying a 5 Ohm-m resistivity layer. This low-resistivity layer is an indication of high clay content. In the far northeast in the Cieneguita cienegas complex, Z3/H8 displays at the surface a resistivity of 5 Ω -m layer underlain by a 20-50 Ohm-m resistivity layer. This low 5 Ohm-meter resistivity layer indicates a thin layer of clay-rich material at the surface, which agrees with conditions noted in the field. The deeper resistivities at this site are consistent with normal alluvium resistivities.

Induced polarization (IP) surveys were conducted by Zonge International Inc., as described in Chapter 3. No IP information was collected by HGI Inc., because of large EM coupling within the transmitter/receiver cable. More modeling of the IP data is needed in order to interpret the IP data. The Zonge International IP data may also be largely affected by EM coupling.

7.1. Possible Future Surveys

The dense multiple-electrical-sounding profiles that were used in this project showed reasonably homogenous resistivities along each profile. There were large changes in resistivity between some of the profile locations. Therefore, future work may be most efficient if single electrical soundings were used instead of dense multiple-electrical-soundings along a profile. This would make it possible to map the regional variations in resistivity over a larger area.

Although airborne EM surveys involve a large mobilization cost, the cost per measurement point along each flight line can be low. This would allow detailed mapping of the regional resistivity variations, if sufficient funds were available for an airborne EM survey.

8. Acknowledgements

The University of Arizona Geophysics Field Methods class, GEN/GEOS 416/516, would like to thank the Bureau of Land Management (BLM) and the Nature Conservancy for providing funding and support for this project. Specifically, we would like to thank Jeanmarie Haney and Gita Bodner of The Nature Conservancy and Ben Lomeli of the Bureau of Land Management for organizing and coordinating the project. Without these sources of funding and support, the class would not have been possible this year.

Zonge International provided the equipment and training necessary to conduct the first half of the data collection as well as modelling the data. Scott Urquhart, President of Zonge, and Anna Szidarovsky, Project Geophysicist at Zonge, provided excellent hands-on training to operate the GDP-32 as well as to properly set up a complex resistivity line. Additionally, Anna spent large amounts of extra time explaining processing methods and working on the data processing personally. Wanjie Feng, Geophysicist at Zonge, provided additional support in both training and operating the instrumentation in the field during one of the weekends and during the training exercises, providing essential assistance in our data collection. Zonge international has played a vital role in the field camp this year and indeed nearly every year for the last 30 years. We greatly appreciate their continued assistance in allowing students to directly experience modern geophysical methods.

Hydrogeophysics, Inc. (HGI) provided equipment and training for the second half of data collection as well as data modelling and interpretation. Dale Rucker, the Chief Technical Officer of HGI, spent time in the field during the weekend to collect seven full resistivity lines. Along with his personal assistance in the field, he gave a thorough explanation of different arrays and some of the mathematical operations involved with each of them. After the data were collected, he opened his office up to us and lent us both hardware and software to use in order to process the data. Once the data were processed correctly, he also assisted in the interpretation.

The class would like to thank personnel from the Las Cienegas National Conservation Area for allowing us to have full access to the site. Additionally, we would like to thank the United States

Geologic Survey (USGS) for publishing large amounts of publicly available data, which were highly relevant to this project.

9. References

“DC Resistivity & Electrical Resistivity Tomography (ERT).” *Zonge.com*. Trusted Geophysics. Zonge International 2017. Web. 24 February 2017.

Cubbage, B., Noonan, G.E., Rucker, D. F., 2017. Modified Wenner Array for Efficient use of 8-Channel Resistivity Meters, *Pure and Applied Geophysics*.

Gasperikova, E., and Morrison, F., 2016. DC Electric Methods, *The Berkeley Course in Applied Geophysics*, <http://appliedgeophysics.berkeley.edu/dc/index.html> (April 16, 2017).

Kearey, P., Brooks, M., and Hill, I., 2002. *An Introduction to Geophysical Exploration, 3rd Edition*. Hoboken, New Jersey, 272p.

Sharma, P. V. *Geophysical Methods in Geology*. New York: Elsevier, 1986. Print.

U.S. Army Corps of Engineers, 1995. *Geophysical Exploration for Engineering and Environmental Investigations*. 208p.